

Integrative decomposition of multi-source data by identifying partially-joint score subspaces

SeoWon Choi^a, Sungkyu Jung^{a,1}

^a*Department of Statistics, Seoul National University, Seoul, Republic of Korea*

Abstract

Analysis of multi-source dataset, where data on the same objects are collected from multiple sources, is of rising importance in many fields, most notably in multi-omics biology. We propose a novel framework and algorithms for integrative decomposition of such multi-source data, to identify and sort out common factor scores in terms of whether the scores are relevant to all data sources (fully joint), to some data sources (partially joint), or to a single data source. The key difference between our proposal and existing approaches is that we utilize raw source-wise factor score subspaces in the identification of the partially-joint block-wise association structure. To identify common score subspaces, which may be partially joint to some of data sources, from noisy observations, our proposed algorithm sequentially computes one-dimensional flag means among source-wise score subspaces, then collects the subspaces that are close to the mean. The proposed decomposition boasts fast computational speed, and is superior in identifying the true partially-joint association structure and recovering the joint loading and score subspaces than competing approaches. The proposed method is applied to a blood cancer multi-omics data set, containing measurements from three data sources. We identify a latent score, partially joint to the drug panel and methylation profile data sources but not relevant to RNA sequencing profiles, that helps discovering hidden clusters in the data.

Keywords: Multi-block data, Factor model, Principal angles, Data integration, Dimension reduction

¹This work was supported by Samsung Science and Technology Foundation under Project Number SSTF-BA2002-03.

1. Introduction

In various fields of science and technology, there is a growing interest in analyzing multi-source data in an integrative way. By the *multi-source data*, we mean data obtained for multiple groups of variables on the same set of subjects. Each group of variables is observed from a common source, and form a data block. A prominent example of multi-source data is modern multi-omics data that include gene expressions, RNA sequencing, mutations, epigenetic markers or metagenomic materials (Subramanian et al., 2020). The recent development of high-throughput technologies enables us to extract these sources of information comprehensively from a given preparation of cancer/normal tissue samples (Reuter et al., 2015; Norris et al., 2017).

One of the main challenges in analyzing multi-omics data is that data blocks come from distinct measurements of different sources. For example, our motivating data set consists of three data blocks, each from a drug response panel, genome-wide DNA methylation profiles and RNA sequencing profiles (Dietrich et al., 2018); see Section 6 for a detailed description of the data. Separately analyzing each data block hinders the assessment of inter-relations among different data blocks. To capture the potentially joint association structures in these multi block data, the *linked component model* has been oftentimes used (Smilde et al., 2003; VanDeun et al., 2009; Lock et al., 2013).

Suppose that there are K data blocks, $X_k \in \mathbb{R}^{p_k \times n}$, for $k = 1, \dots, K$, observed for n subjects. The subjects in the data are common and matched, i.e., the measurements for the i th subject appear in the i th column of each data matrix. Assuming zero mean, each data block is decomposed into

$$X_k = Z_k + E_k = U_k V_k^T + E_k, \quad k = 1, \dots, K, \quad (1)$$

in which the low-rank “signal” matrix Z_k is factored into a loading matrix U_k and a score matrix V_k . The linked component model further assumes that two or more data blocks can potentially share a common score component (VanDeun et al., 2009). An extreme example is that all scores are common to all data blocks, that is, $V_1 = \dots = V_k$, as in Smilde et al. (2003). The models considered in Lock et al. (2013) and Feng et al. (2018) allow some scores to be common to all data blocks, explaining the joint variation among all data blocks, and some scores to be specific to each data blocks (explaining the individual variations in a single data block).

Following Gaynanova and Li (2019) and Gao et al. (2021), we in addition allow *partially-joint* scores that are shared across multiple, but not necessarily all, data blocks. An illustrative example of such a model, for $K = 3$ blocks of data, is $(X_1^T, X_2^T, X_3^T)^T = UW^T + E$,

$$UW^T = \begin{pmatrix} U_{(1),1} & U_{(1),2} & 0 \\ U_{(2),1} & U_{(2),2} & 0 \\ U_{(3),1} & 0 & U_{(3),3} \end{pmatrix} (W_{\{1,2,3\}} \quad W_{\{1,2\}} \quad W_{\{3\}})^T, \quad (2)$$

where U is the loading matrix, $W_{\{1,2,3\}}$ is a matrix of scores that affect all data blocks, and $W_{\{1,2\}}$ is a partially-joint score matrix, affecting only the first two data blocks, but not the third. The scores in $W_{\{3\}}$ are specific to the third data block. Our goal is to delineate such an association structure from a multi-source data.

In this paper, we develop a novel framework and estimation strategy for integrative decomposition of multi-source data, by identifying scores that are fully joint to all data sources, partially joint to some, or specific to a single data source. The framework utilizes the signal score subspace $[V_k]$, a rank r_k subspace of \mathbb{R}^n , spanned by the columns of the signal matrix Z_k in (1). The rationale for using $[V_k]$ is straightforward: If a common score of rank r is shared by the first two data blocks, then the intersection of $[V_1]$ and $[V_2]$ is non-empty, and is a dimension r subspace. To capture the partially-joint block-wise association structure from the score subspaces $[V_k]$, we define the collection of triples

$$\mathfrak{S} := \mathfrak{S}(\{[V_k]\}_{k=1,\dots,K}) = \{(S, r(S), [W_S]) : S \subset \mathcal{K}\},$$

in which a non-empty subset S of $\mathcal{K} = \{1, \dots, K\}$ denotes a specific pattern of block-wise association, W_S denotes the corresponding common scores (that are either fully-joint, partially-joint or specific to data sources) of rank $r(S)$. See Section 2 for a detailed construction of \mathfrak{S} , and Section 4 for conditions to guarantee the uniqueness of \mathfrak{S} .

To identify the partially-joint score structure \mathfrak{S} from noisy observations, we propose to compute the flag mean of signal subspaces (Draper et al., 2014), and to test whether the mean is indeed close to signal subspaces. If a mean w is “close” to $[V_1]$ and $[V_2]$, but not to other subspaces, then it is a basis of (estimated) $W_{\{1,2\}}$. We use a tunable parameter to determine the closeness between two subspaces. The algorithm, detailed in Section 3, is quick in decomposing multi-source data sets, and boasts a superior performance in

identifying \mathfrak{S} and in the estimation of the subspaces spanned by the loading matrices and by the common score matrices.

Recently, there has been a growing interest in integrative decomposition of multi-source data (Lock et al., 2013; Li and Jung, 2017; Feng et al., 2018; Li and Gaynanova, 2018; Gaynanova and Li, 2019; Gao et al., 2021). Among these, Gaynanova and Li (2019) and Gao et al. (2021) also considered modeling partially-joint association structures. However, these authors focused on the loading matrix U , and exploited the source-wise sparse structure of the matrix U , as seen in (2). On the contrary, we explicitly utilize the signal score matrices V_k in (1) in identifying partially-joint scores of (2). The loading matrix is naturally obtained as a subsequent step in our proposal. Our approach extends the angle-based joint and individual variation identification of Feng et al. (2018), in which partially joint variations were not considered. In Section 5, we numerically confirm that our proposal finds the true association structure much more accurately than the aforementioned decomposition methods.

The rest of article is organized as follows. In Section 2, we formally present our integrative decomposition framework and define the partially joint structure \mathfrak{S} , followed by the proposed decomposition algorithm and tuning parameter selection procedure in Section 3. In Section 4, conditions to guarantee unique decompositions are discussed. Section 5 is devoted to numerical illustrations and comparisons to existing methods. In Section 6, we demonstrate the use of the proposed method in an analysis of a blood cancer multi-omics data set associated with drug responses, and reveal that the proposal detects a latent signal pattern, partially joint across two, but not all, data sources, which is not easily seen by a separate analysis of individual data blocks. Proofs, technical lemmas, examples and extended numerical results are given in the supplementary material.

2. Statistical framework

Consider a set of data matrices $X_k \in \mathbb{R}^{p_k \times n}$ for $k = 1, \dots, K$, where the i th column of each data matrix corresponds to the same (i th) subject. We assume that each X_k is additively decomposed into the rank r_k true signal matrix Z_k and random errors E_k so that $X_k = Z_k + E_k$. Assuming $n > r_k$, the true signal matrix $Z_k = U_k V_k^T$ is further factored into the factor loading matrix $U_k \in \mathbb{R}^{p_k \times r_k}$ and the factor score matrix $V_k \in \mathbb{R}^{n \times r_k}$, where V_k is normalized to satisfy $V_k^T V_k = I_{r_k}$. In our development of partially-joint

structure identification, the rank- r_k subspace of \mathbb{R}^n , spanned by the columns of V_k , plays an important role. We denote $[V_k]$ for the column space of V_k , and call it (true) *signal score subspace* for the k th data block.

2.1. Partially-joint structures

Note that all signal score subspaces $[V_1], \dots, [V_k]$ are subspaces of \mathbb{R}^n . If, say, $[V_1]$ and $[V_2]$ overlap, then the corresponding data blocks (X_1, X_2) share a common score, represented by the subspace $[V_1] \cap [V_2]$, which is at least partially-joint to data blocks X_1 and X_2 . However, if in addition $[V_1] \cap [V_2] \subset [V_3]$, then the common score is not only relevant to X_1 and X_2 , but also relevant to all three blocks. To identify and index score subspaces according to whether the score subspaces are *fully-joint* (relevant to all K data blocks), *partially-joint* (relevant to some but not all data blocks), or specific to each data block, we use a sequential approach, as described below.

Let $\mathcal{K} = \{1, \dots, K\}$ be the index set of K data blocks, and consider a partially ordered set $(\mathcal{2}^{\mathcal{K}} \setminus \{\phi\}, \subset)$ in which the order is given by the set-inclusion relation. An example of $\mathcal{2}^{\mathcal{K}} \setminus \{\phi\}$ is given in Fig. 1, for the case $K = 3$. We index all $2^K - 1$ elements of $(\mathcal{2}^{\mathcal{K}} \setminus \{\phi\}, \subset)$ so that $S_i, S_j \in \mathcal{2}^{\mathcal{K}}$, $i, j \in \mathcal{I}_K = \{1, \dots, 2^K - 1\}$, satisfies

$$|S_i| \geq |S_j| \iff i < j, \quad (3)$$

where $|S|$ is the number of elements in the set S . For example, for $K = 3$, $S_1 = \{1, 2, 3\}$ as appeared in the top row of Fig. 1, and the next three sets (S_2, S_3, S_4) are given by the next row of the figure. That is, S_2, S_3 , and S_4 are $\{1, 2\}, \{2, 3\}, \{1, 3\}$, respectively. Likewise, $S_5 = \{1\}, S_6 = \{2\}, S_7 = \{3\}$. Each element S_i stands for the indices of data blocks that potentially possess a common score. Of course, such indexing is not unique, and one may set, e.g., $S_6 = \{3\}, S_7 = \{2\}$. Conditions to guarantee invariance of the decomposition with respect to different choices of indexing will be discussed in Section 4. For now, assume that an order is given to the elements of the set $\mathcal{2}^{\mathcal{K}} \setminus \{\phi\}$, and satisfies (3).

The indexed partially-ordered set $(\mathcal{2}^{\mathcal{K}} \setminus \{\phi\}, \subset)$ provides the bare structure to which we identify the association among K data sources. We begin with identifying the fully-joint score subspace, corresponding to the first index set $S_1 = \{1, 2, \dots, K\}$. The fully-joint score subspace, denoted by $[W_1]$, is

$$[W_1] := \bigcap_{k \in S_1} [V_k].$$

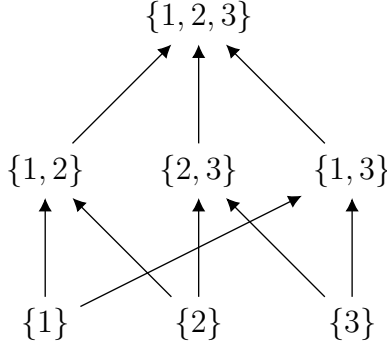


Figure 1: An example of ordering in the indexed partially-ordered set $(\mathcal{2}^{\mathcal{K}} \setminus \{\phi\}, \subset)$, where $\mathcal{K} = \{1, 2, 3\}$, and arrow \rightarrow stands for \subset , e.g. $\{1\} \rightarrow \{1, 2\}$ means $\{1\} \subset \{1, 2\}$.

Next, the partially joint score subspace corresponding to data blocks indexed by S_2 is identified. Note that the common score subspace corresponding to S_2 , $\cap_{k \in S_2} [V_k]$, already contains $[W_1]$, thus we are only interested in the orthogonal complement of $[W_1]$ in \mathbb{R}^n . Writing P_j^\perp for the projection transformation of \mathbb{R}^n onto the orthogonal complement of $[W_j]$, we define

$$[W_2] := P_1^\perp (\cap_{k \in S_2} [V_k]).$$

In general, for $i \in \mathcal{I}_K$, define the partially-joint score subspace $[W_i]$ corresponding to $S_i \in (\mathcal{2}^{\mathcal{K}} \setminus \{\phi\}, \subset)$ in a recursive manner:

$$[W_i] := \left(\bigcirc_{\substack{\{j: j < i, \\ S_j \cap S_i \neq \phi\}}} P_j^\perp \right) (\cap_{k \in S_i} [V_k]), \quad (4)$$

where the notation $\bigcirc_{j \in J} P_j^\perp([A])$, for an indexed set $J \subset \mathcal{I}_K$ and a subspace $[A]$, stands for the repeated applications of P_j^\perp on $[A]$, where P_j^\perp s are applied one by one by the increasing order of $j \in J$. Note that depending on $\{[V_k]\}$, a $[W_i]$ may be $\{0\}$.

Example 2.1. Suppose $K = 3$, and that $(\mathcal{2}^{\mathcal{K}} \setminus \{\phi\}, \subset)$ is indexed as in Fig. 1. Then, as an instance, for $i = 6$, $S_6 = \{2\}$, the set $\{S_j : j < 6, S_j \cap S_6 \neq \phi\}$, used in (4), contains three elements $\{2, 3\}, \{1, 2\}, \{1, 2, 3\}$, which can be found by following the arrows stemming from $S_6 = \{2\}$ in Fig. 1.

Given the ordered index-sets $S_i \in (\mathcal{2}^{\mathcal{K}} \setminus \{\phi\}, \subset)$, $i \in \mathcal{I}_K$, we call $[W_i]$ the *partially-joint score subspace* corresponding to the data blocks indexed by S_i .

Note that for $i = 1$, $[W_i]$ is indeed the fully-joint score subspace. For the last K elements of \mathcal{I}_K , it is in fact the score subspace specific to each data source, which might be called an *individual* score subspace, as in Lock et al. (2013) and Feng et al. (2018). Nevertheless, for simplicity, we call $[W_i]$ partially-joint, in which the *part* can be the whole or individuals. Denoting $r(S_i)$ for the dimension of $[W_i]$, the *partially-joint block-wise association structure* of the true signal matrices is the collection of triples

$$\mathfrak{S} = \mathfrak{S}(\{Z_k\}_{k \in \mathcal{K}}) := \{(S_i, r(S_i), W_i) : i \in \mathcal{I}_K\}.$$

The elements in \mathfrak{S} represent the patterns of association among the data blocks. For example, the triple $(\{1, 2\}, 2, [w_1, w_2])$ means that there are two dimensional factor scores $[w_1, w_2] \in \mathbb{R}^{n \times 2}$, shared only by the first and second data sources, while $(\{2, 3\}, 0, \{0\})$ means that there is no common score relevant only to the second and third data sources.

For ease of notation, we also write W_{S_i} for W_i (and $[W_{S_i}]$ for $[W_i]$). The collection exploits all of the signal score subspaces, that is, $+_{i \in \mathcal{I}_K} [W_i] = +_{k \in \mathcal{K}} [V_k]$, where the notation ‘+’ means the sum of subspaces, and

$$+_{i \in \{k \in S_i\}} [W_{S_i}] = [V_k], \quad (5)$$

as shown in Lemma A.3 in the supplementary material. We also note that for any $i \neq j$, $[W_i]$ and $[W_j]$ do not overlap, i.e., $[W_i] \cap [W_j] = \{0\}$, but they are not necessarily orthogonal. However, if both $[W_i]$ and $[W_j]$ are related to a common data source, then they are orthogonal, as shown below.

Lemma 2.1. *For $i, j \in \mathcal{I}_K$ and $S_i \cap S_j \neq \emptyset$, $[W_i] \perp [W_j]$.*

As an instance, $[W_{\{1\}}]$ is orthogonal to $[W_{\{1,2\}}]$ and to $[W_{\{1,2,3\}}]$, but may not be orthogonal to either $[W_{\{2,3\}}]$, $[W_{\{2\}}]$, or $[W_{\{3\}}]$. Moreover, for each $k = 1, \dots, K$, Lemma 2.1 ensures that all partially-joint score subspaces relevant to the k th data block, $\{[W_{S_i}] : k \in S_i, i \in \mathcal{I}_K\}$, are orthogonal to each other. Thus, the subspaces in the left hand side of (5) are indeed orthogonal to each other.

2.2. Partially-joint score and loading matrices

Given $\mathfrak{S} = \{(S_i, r(S_i), [W_i]) : i \in \mathcal{I}_K\}$, for each i satisfying $r(S_i) > 0$, fix an orthogonal basis $W_i \in \mathbb{R}^{n \times r(S_i)}$ of $[W_i]$. The potentially joint scores in

the matrix $W_i \in \mathbb{R}^{n \times r(S_i)}$ are linked to the signal matrix $Z_k \in \mathbb{R}^{p_k \times n}$ via its corresponding *loading matrix*

$$U_{(k),i} := Z_k W_i \in \mathbb{R}^{p_k \times r(S_i)},$$

for $k = 1, \dots, K$, and $i \in \mathcal{I}_K$, provided that $r(S_i) > 0$. If $r(S_i) = 0$, then there is no need to define a loading matrix. It can be checked that the signal score matrix Z_k is additively decomposed into

$$Z_k = \sum_{i \in \mathcal{I}_{(k)}} U_{(k),i} W_i^T, \quad (6)$$

where $\mathcal{I}_{(k)} = \{i : k \in S_i\} \subset \mathcal{I}_K$ collects all indices relevant to the k th block. The partially-joint score matrices appearing in the decomposition (6) are orthogonal to each other.

We emphasize that if $k \notin S_i$, then $U_{(k),i} = 0_{p_k \times r(S_i)}$. In other words, the partially-joint loading matrix $U_{(k),i}$ is zero if the corresponding partially-joint scores W_i are not relevant to the k th data block. An example elucidating this point is given below.

Example 2.2. Suppose $K = 3$, and that $(\mathfrak{2}^{\mathcal{K}} \setminus \{\phi\}, \subset)$ is indexed as in Fig. 1. Further suppose that $W_1 = W_{\{1,2,3\}}$, $W_2 = W_{\{1,2\}}$, and $W_7 = W_{\{3\}}$ are each of dimension 1, and all other partially-joint score subspaces are of rank zero. That is, $r(S_1) = r(S_2) = r(S_7) = 1$, and $r(S_i) = 0$ otherwise. Given $X_k = Z_k + E_k$ ($k = 1, 2, 3$), the signal matrices Z_k 's are jointly decomposed into

$$\begin{pmatrix} X_1 \\ X_2 \\ X_3 \end{pmatrix} = \begin{pmatrix} U_{(1),1} & U_{(1),2} & 0 \\ U_{(2),1} & U_{(2),2} & 0 \\ U_{(3),1} & 0 & U_{(3),7} \end{pmatrix} (W_1 \quad W_2 \quad W_7)^T + \begin{pmatrix} E_1 \\ E_2 \\ E_3 \end{pmatrix} =: UW^T + E.$$

It can be seen that the index-set $S_2 = \{1, 2\}$, for example, has the score W_2 , which is related only to the first two blocks, as shown in the second column of U .

The decomposition of Z_k 's into the partially-joint loading and score matrices is not unique. If instead of W_i (and its corresponding loading matrix $U_{(k),i}$, for $k \in \mathcal{K}$, one chooses $W'_i = W_i R$, for an orthogonal matrix R , then the corresponding loading matrix becomes $U'_{(k),i} = U_{(k),i} R$. Nevertheless, if $U_{(k),i}$ is zero, then $U_{(k),i} R$ is zero for any orthogonal R , and the pattern of fully-joint, partially-joint and individual structures is invariant to the choices of basis.

3. Estimation

In practice, the signal Z_k and error E_k of data matrices $X_k \in \mathbb{R}^{p_k \times n}$ for $k = 1, \dots, K$ are unknown. We assume that the ranks r_k of the signal matrices are pre-determined, or pre-estimated via methods for estimating the number of factors or principal components (see e.g. Bai and Ng (2002); Passemier and Yao (2014); Jung et al. (2018) and references therein). We extract the signal matrix using a low-rank approximation of X_k , and write the rank r_k approximation of X_k by \widehat{Z}_k . While we have used the rank r_k singular value decomposition applied to (centered) X_k to obtain \widehat{Z}_k , but one may use any off-the-shelf factor model estimator to obtain \widehat{Z}_k . The basis of the signal score subspace \widehat{V}_k is given either by the right singular vectors of Z_k or by the factor model estimates.

We iterate through all index-sets $S_i \in (\mathcal{2}^{\mathcal{K}} \setminus \{\phi\}, \subset)$ for $i = 1, \dots, 2^K - 1$, by increasing order. At the i th step, our goal is to obtain the partially-joint score subspace estimate $[\widehat{W}_i]$ from $\{[\widehat{V}_k]\}_{k \in S_i}$. If $[\widehat{V}_k]$'s were free from noises, i.e., $[\widehat{V}_k] = [V_k]$, then we would evaluate the intersection of $[\widehat{V}_k]$'s, as in (4). However, since \widehat{Z}_k is contaminated with noises, we may have $\cap_{k \in S_i} [\widehat{V}_k] = \{0\}$ even if $\cap_{k \in S_i} [V_k] \neq \{0\}$. Thus, there is a need to give a slack on identifying the “intersection” of $[V_k]$'s, accounting for random perturbations in $[\widehat{V}_k]$. We propose to use principal angles between subspaces for such identification, further developed in Section 3.1.

In Section 3.1, we propose a procedure that finds a basis matrix \widehat{W}_i for the partially-joint score subspace estimate $[\widehat{W}_i]$ at each i th step. The rank of the corresponding S_i is set as $\hat{r}(S_i) = \text{rank}(\widehat{W}_i)$. After estimating \widehat{W}_i and $\hat{r}(S_i)$, we move on to the next step for S_{i+1} . Finishing the iteration over all S_i 's by the order specified in $(\mathcal{2}^{\mathcal{K}} \setminus \{\phi\}, \subset)$, an estimated partially-joint structure $\widehat{\mathfrak{S}} = \{(S_i, \hat{r}(S_i), \widehat{W}_i) : i \in \mathcal{I}_K\}$ is obtained.

Given $\widehat{\mathfrak{S}}$, we then discuss the estimation of corresponding partially-joint loading matrices in Section 3.2, followed by a discussion on the strategy of thresholding at the right principal angle in Section 3.3.

3.1. Partially-joint Score Subspace Estimation

The triples $(S_i, r(S_i), W_i)$ in \mathfrak{S} are estimated sequentially for $i = 1, \dots, 2^K - 1$. At the i th stage, we work with the index-set $S_i \subset \{1, \dots, K\}$, and estimate the partially-joint score subspace $[W_i]$ by collecting one-dimensional bases, that lie “close” to each and every score subspaces in $\{[\widehat{V}_k]\}_{k \in S_i}$. For the notion of closeness, we use a threshold parameter $\lambda \in [0, \pi/2)$ for the principal

Algorithm 1: Partially-joint Structure Identification

input: $\widehat{V}_1, \dots, \widehat{V}_K, \lambda$
for $i = 1, 2, \dots, 2^K - 1$ **do**
 Set $\mathcal{W}_i = \phi$;
 while $\dim([\widehat{V}_k]) > 0$ for all $k \in S_i$ **do**
 (a) Compute the mean direction \hat{w} (7) of $\{[\widehat{V}_k]\}_{k \in S_i}$;
 if the condition (8) is satisfied **then**
 (b) Let $\mathcal{W}_i \leftarrow \mathcal{W}_i \cup \{\hat{w}\}$;
 (c) Update $\widehat{V}_k \leftarrow \widehat{V}_{k, trunc}$ for each $k \in S_i$
 else
 | break;
 end
 end
 Let $\hat{r}(S_i) = |\mathcal{W}_i|$, write \widehat{W}_i for the $n \times \hat{r}(S_i)$ matrix consisting of elements in \mathcal{W}_i and record $(\widehat{S}_i, \hat{r}(S_i), \widehat{W}_i)$ in $\widehat{\mathfrak{S}}$;
end
Result: $\widehat{\mathfrak{S}}$

angle between subspaces. For now, λ is treated as a pre-determined tuning parameter, and a data-driven choice of λ will be discussed in Section 3.3. Our algorithm for computing \widehat{W}_i consists of an iterative application of three steps, labeled (a)—(c).

Briefly, Step (a) finds a *mean direction* that lies closest to all score subspaces $\{[\widehat{V}_k]\}_{k \in S_i}$, as a candidate that may be included in \widehat{W}_i . Step (b) tests whether the mean direction is indeed close to each and every member in $\{[\widehat{V}_k]\}_{k \in S_i}$. If so, then the mean direction contributes to \widehat{W}_i and each $[\widehat{V}_k]$ is deflated in Step (c), so that the next mean direction is orthogonal to previous ones. The procedure is repeated until there is no more mean direction accounted for \widehat{W}_i . The mean directions included in \widehat{W}_i are orthogonal to each other, and $\hat{r}(S_i) = \text{rank}(\widehat{W}_i)$ is simply the number of mean directions collected.

Algorithm 1 summarizes the proposed partially-joint structure identification procedure, using steps (a)—(c). Details of the three steps are given below. Throughout the process, $[\widehat{V}_k]$'s are deflated iteratively and can become the zero-dimensional subspace denoted by $\{0\}$. The following is applied

sequentially for $i = 1, \dots, 2^K - 1$. At the i th stage, we begin with $\mathcal{W}_i = \emptyset$, to which the identified one-dimensional bases of the partially-joint score subspace are added. Recall that $\lambda \in [0, \pi/2)$ is given.

- (a) As a candidate for a basis vector of the partially joint score matrix, compute the mean direction \hat{w} among $\{[\hat{V}_k]\}_{k \in S_i}$, provided that $[\hat{V}_k] \neq \{0\}$ for all $k \in S_i$. The mean direction minimizes the sum of the squares of the subspace distances between a candidate w and subspaces $[\hat{V}_k]$ for $k \in S_i$, and is

$$\hat{w} = \operatorname{argmin}_{w^T w = 1} \sum_{k \in S_i} d([w], [\hat{V}_k])^2, \quad (7)$$

where $d([w], [B]) = 1/\sqrt{2} \cdot \|ww^T - BB^T\|_F$ is the Frobenius-norm distance between subspaces $[w]$ and $[B]$ (Ye and Lim, 2016). We chose the Frobenius norm, since for any choice of the basis \hat{V}_k for $[\hat{V}_k]$,

$$\sum_{k \in S_i} d([w], [\hat{V}_k])^2 = |S_i| - w^T \left(\sum_{k \in S_i} \hat{V}_k \hat{V}_k^T \right) w = |S_i| - w^T (H H^T) w,$$

where H is the matrix given by the column-wise binding of \hat{V}_k 's (Draper et al., 2014), and \hat{w} is the first left singular vector of H . We mention in passing that $[\hat{w}]$ is the one-dimensional flag mean of subspaces $\{[\hat{V}_k]\}_{k \in S_i}$ (Draper et al., 2014).

- (b) Check whether all of the signal score subspaces $[\hat{V}_k]$ are not too dispersed from \hat{w} (7). For this, given the prespecified λ , we check whether the *principal angle* between the mean direction and each of $[\hat{V}_k]$ is at most λ , i.e.,

$$d([\hat{w}], [\hat{V}_k]) < \sin(\lambda), \quad \text{for all } k \in S_i. \quad (8)$$

Here, the principal angle $\theta([w], [B]) := \arcsin(d([w], [B])) \in [0, \pi/2]$ is the acute angle formed by the vector w and the subspace $[B]$ (Björck and Golub, 1973). If the condition (8) is not satisfied, then skip the following and move to the next stage for S_{i+1} . If (8) is satisfied, then \mathcal{W}_i is updated to $\mathcal{W}_i \leftarrow \mathcal{W}_i \cup \{\hat{w}\}$.

- (c) The basis \hat{w} , that has been added to \mathcal{W}_i , is now “removed” from each of $[\hat{V}_k]$, $k \in S_i$. Since \hat{w} is not exactly in $[\hat{V}_k]$, the one-dimensional subspace

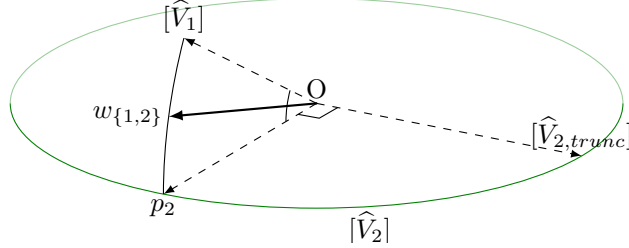


Figure 2: A figurative description for computing partially-joint score subspace $[\widehat{W}_i]$, for $S_i = \{1, 2\}$. The two-dimensional subspace $[\widehat{V}_2]$ is depicted as a disk. $w_{\{1,2\}}$ is the mean direction and p_2 stands for the projection of $w_{\{1,2\}}$ onto $[\widehat{V}_2]$.

closest to \hat{w} is removed. Specifically, let $[\widehat{V}_{k, trunc}]$ be the orthogonal complement of $P_{\widehat{V}_k} \hat{w}$ within $[\widehat{V}_k]$. (Note that $\dim([\widehat{V}_{k, trunc}]) = \dim([\widehat{V}_k]) - 1$.) Write $[\widehat{V}_k]$ for $[\widehat{V}_{k, trunc}]$, for each $k \in S_i$. If any $[\widehat{V}_k]$ for $k \in S_i$ becomes $\{0\}$, then move to the next stage for S_{i+1} . Otherwise, move back to step (a).

We give an illustrative example for the three steps.

Example 3.1. *Suppose for simplicity there are three data blocks, and we are at the stage of estimating the partially-joint structure for $S_i = \{1, 2\}$. Assume that $[\widehat{V}_1]$ has been deflated (in the previous stages) to be of dimension 1, while $[\widehat{V}_2]$ is of dimension 2. If in addition the dimension of the score space is $n = 3$, then these signal subspaces can be visualized as done in Fig. 2. There, $[\widehat{V}_1]$ is generated by $(\cos \pi/6, 0, \sin \pi/6)^T$, and $[\widehat{V}_2]$ by $(1, 0, 0)^T$ and $(0, 1, 0)^T$. In Step (a), the mean direction $\hat{w} = (\cos \pi/12, 0, \sin \pi/12)^T$ is computed. Since for $k = 1, 2$, $\theta([\hat{w}], [\widehat{V}_k]) = \pi/12$, (8) is satisfied for any tuning parameter $\lambda > \pi/12$, and we say that $[\widehat{V}_1]$ and $[\widehat{V}_2]$ share a partially-joint score subspace, and \hat{w} is included as a basis of $[W_{\{2,3\}}]$ (in Step (b)). In step (c), $[\widehat{V}_2]$ is updated to $[\widehat{V}_2] \leftarrow [\widehat{V}_{2, trunc}] = \text{span}((0, 1, 0)^T)$, and $[\widehat{V}_1]$ becomes $\{0\}$. Since there is no more scores left to exploit, we move onto the next stage for $S_{i+1} = \{2, 3\}$.*

For a singleton set $S_i = \{k\}$, the mean direction \hat{w} is any unit vector in (the deflated) $[\widehat{V}_k]$, and the condition (8) is always satisfied. Thus, for this case, $\widehat{W}_i = \widehat{V}_k$, in place of steps (a)—(c) above.

The estimated partially-joint score matrices \widehat{W}_i consist of orthogonal columns, and $\widehat{W}_i^T \widehat{W}_i = I_{\hat{r}(S_i)}$. Just like the true partially-joint score subspaces (cf. Lemma 2.1), for i, j satisfying $S_i \cap S_j \neq \emptyset$, $\widehat{W}_j^T \widehat{W}_i = 0$.

3.2. Partially-joint Loading Matrix Estimation

Given the partially-joint structure estimate $\widehat{\mathfrak{S}}(\{\widehat{Z}_k\}_{k \in \mathcal{K}}) = \{(S_i, \hat{r}(S_i), \widehat{W}_i) : i \in \mathcal{I}_K\}$, we obtain the estimated partially-joint loading matrix \widehat{U} . Let $\widehat{Z} = (\widehat{Z}_1^T, \dots, \widehat{Z}_K^T)^T \in \mathbb{R}^{p \times n}$, where $p = \sum_{k=1}^K p_k$. Denote the column-wise concatenation of \widehat{W}_i as $\widehat{W} \in \mathbb{R}^{n \times \hat{r}}$, where $\hat{r} = \sum_{i \in \mathcal{I}_K} \hat{r}(S_i)$. One may naively consider estimating the partially-joint loading matrix from the optimization problem

$$\widetilde{U} = \underset{U \in \mathbb{R}^{p \times \hat{r}}}{\operatorname{argmin}} \|\widehat{Z} - U \cdot \widehat{W}^T\|_F^2. \quad (9)$$

However, the estimate \widetilde{U} obtained from (9) does not exhibit the block-wise sparsity structure inherited from $\widehat{\mathfrak{S}}(\{\widehat{Z}_k\}_{k \in \mathcal{K}})$; for $k \notin S_i$, the corresponding block $\widetilde{U}_{(k)i}$ of the loading matrix \widetilde{U} should be the zero, but is not so in general. Thus we give a constraint to (9) such that U in (9) has the block sparsity structure that corresponds to the estimated partially-joint structure $\widehat{\mathfrak{S}}$. For example, in the setting of Example 2.2, suppose that $[V_k]$'s are replaced by $[\widehat{V}_k]$'s. We constraint the optimization problem (9) so that U has a block sparsity structure

$$\begin{matrix} p_1 \\ p_2 \\ p_3 \end{matrix} \left\{ \begin{array}{c|c|c} \left[\begin{array}{ccc} U_{(1),1} & U_{(1),2} & 0 \\ \hline U_{(2),1} & U_{(2),2} & 0 \\ \hline U_{(3),1} & 0 & U_{(3),7} \end{array} \right] & & \\ & & \end{array} \right\}, \quad (10)$$

as reflected in $\widehat{\mathfrak{S}}$, i.e., for $S_1 = \{1, 2, 3\}$, $S_2 = \{1, 2\}$ and $S_7 = \{3\}$, $\hat{r}(S_1) = \hat{r}(S_2) = \hat{r}(S_7) = 1$, and $\hat{r}(S_i) = 0$ otherwise.

With the block-wise sparse constraint imposed, the objective function (9) for U can be written separately for each data block, i.e.,

$$\|\widehat{Z} - U \cdot \widehat{W}^T\|_F^2 = \sum_{k=1}^K \|\widehat{Z}_k - \sum_{i \in \mathcal{J}(k)} U_{(k)i} \widehat{W}_i^T\|_F^2 \quad (11)$$

where $\mathcal{J}_{(k)} = \{i : k \in S_i \text{ and } \hat{r}(S_i) > 0\}$. Recall that for each k , the orthogonal matrices \widehat{W}_i , satisfying $i \in \mathcal{J}_{(k)}$, are orthogonal to each other. Thus, provided that $\hat{r}(S_i) > 0$, the minimizer $\widehat{U}_{(k)i}$ of (11) is simply

$$\widehat{U}_{(k)i} = \widehat{Z}_k \widehat{W}_i, \quad \text{for } i, k \text{ satisfying } k \in S_i.$$

By the constraint imposed, $\widehat{U}_{(k)i} = 0$ if $k \notin S_i$. The estimated partially-joint loading matrix consists of $\widehat{U}_{(k)i}$, and is denoted by $\widehat{U} \in \mathbb{R}^{p \times \hat{r}}$, where $p = p_1 + \dots + p_K$.

3.3. Tuning Parameter Selection

The partially-joint structure identification, proposed in Section 3.1, depends heavily on the tuning parameter $\lambda \in [0, \pi/2)$. If λ is too small, then all scores are identified as individual scores, specific to each data blocks. If λ is too large, then individual and partially-joint scores may be falsely identified as fully-joint scores.

We use data splitting to select the value of tuning parameter $\lambda \in [0, \pi/2)$. The signal rank r_k for each dataset X_k is determined using the whole data. For a single instance of data splitting, split n samples of $X = [X_1^T, \dots, X_K^T]^T$ into two groups of equal proportions, the training set $X_{tr} = [X_{tr,1}^T, \dots, X_{tr,K}^T]^T$ and the test set $X_{test} = [X_{test,1}^T, \dots, X_{test,K}^T]^T$. We then extract the training signal matrices $\widehat{Z}_{tr,k}$ for $k = 1, \dots, K$ using the rank r_k approximation of $X_{tr,k}$. Write \widehat{Z}_{tr} for $\{\widehat{Z}_{tr,k} : k = 1, \dots, K\}$. Given a grid of λ 's, we identify the partially-joint structure $\mathfrak{S}(\lambda; \widehat{Z}_{tr})$ that depends on λ , and obtain the partially-joint loading matrix $\widehat{U}_{tr,\lambda}$, as discussed in Sections 3.1 and 3.2.

To assess the degrees to which the estimates are generalized to the test set, we first evaluate the score matrix for the test set, given by $\widehat{U}_{tr,\lambda}$. The test score matrix $\widehat{W}_{test,\lambda}$ is defined as the minimizer $W \in \mathbb{R}^{n_{test} \times \hat{r}}$ of $\|X_{test} - \widehat{U}_{tr,\lambda} W^T\|_F^2$ subject to $W^T W = I_{\hat{r}}$. The test score matrix is computed as $\widehat{W}_{test,\lambda} = P_\lambda Q_\lambda^T$, where P_λ and Q_λ are left and right singular vector matrices of $X_{test}^T \cdot \widehat{U}_{tr,\lambda} = P_\lambda \Sigma_\lambda Q_\lambda^T$, using the Eckart-Young theorem (Eckart and Young, 1936).

Let $\tilde{\lambda}_0$ be the value of λ for which the minimum of the empirical risk is attained. The empirical risk, defined for $\lambda \in [0, \pi/2]$, is

$$\text{Risk}(\lambda) = \sum_{k=1}^K \frac{\|X_{test,k} - \widehat{U}_{tr,\lambda,(k)} \widehat{W}_{test,\lambda}^T\|_F^2}{\|X_{test,k}\|_F^2}, \quad (12)$$

where $\widehat{U}_{tr,\lambda,(k)}$ is the k th row block of $\widehat{U}_{tr,\lambda}$. A similar form was used in Gaynanova and Li (2019). The corresponding partially-joint structure is $\widehat{\mathfrak{S}}(\tilde{\lambda}_0; \widehat{Z}_{tr})$.

It turns out that simply using the tuning parameter $\tilde{\lambda}_0$ for the decomposition of the whole data does not perform well. To be specific, for a given \mathfrak{S} , write

$$\mathfrak{S}_0 = \{(S_i, r(S_i)) : (S_i, r(S_i), W_i) \in \mathfrak{S}, r(S_i) > 0\}.$$

The estimated ranks $\hat{r}(S_i)$ of partially-joint score subspaces from the training data can be very different from those estimated from the whole data, even if we use the fixed $\tilde{\lambda}_0$ for both decompositions. That is, $\widehat{\mathfrak{S}}_0(\tilde{\lambda}_0; \widehat{Z}_{tr})$ is oftentimes different from $\widehat{\mathfrak{S}}_0(\tilde{\lambda}_0; \widehat{Z})$.

On the other hand, the partially-joint structure identified by $\widehat{\mathfrak{S}}(\tilde{\lambda}_0; \widehat{Z}_{tr})$ generalizes well to the whole data. Thus, rather than simply using the chosen λ_0 (and in turn $\widehat{\mathfrak{S}}(\tilde{\lambda}_0; \widehat{Z})$ for the whole data), we use the structure $\widehat{\mathfrak{S}}_0(\tilde{\lambda}_0; \widehat{Z}_{tr})$ in choosing the tuning parameter $\hat{\lambda}$ for the whole data. For this purpose, we use a measure of dissimilarity between the two partially-joint structures, denoted by

$$\text{diff}(\mathfrak{S}_0, \mathfrak{S}'_0), \quad (13)$$

which will be defined shortly. To decompose the whole data X_1, \dots, X_K , for each candidate λ , the partially-joint structure $\widehat{\mathfrak{S}}(\lambda; \widehat{Z})$ from the whole data is identified. We set the value of λ (or, rather choose the structure imposed by $\widehat{\mathfrak{S}}(\lambda; \widehat{Z})$) to be

$$\hat{\lambda} = \underset{\lambda}{\text{argmin}} \text{diff} \left(\widehat{\mathfrak{S}}_0(\tilde{\lambda}_0; \widehat{Z}_{tr}), \widehat{\mathfrak{S}}_0(\lambda; \widehat{Z}) \right),$$

where $\tilde{\lambda}_0$ is the cross-validated choice, minimizing (12). In all numerical examples, we use $\hat{\lambda}$, $\widehat{\mathfrak{S}}(\hat{\lambda}; \widehat{Z})$, and the corresponding partially-joint loading matrix.

The measure of dissimilarity $\text{diff}(\mathfrak{S}_0, \mathfrak{S}'_0)$ is now defined. Let $d_p : (\mathcal{2}^{\mathcal{K}} \setminus \{\phi\}) \times (\mathcal{2}^{\mathcal{K}} \setminus \{\phi\}) \rightarrow \{0, 1, \dots, K\}$ be defined as $d_p(S_i, S_j) = |S_i \Delta S_j|$, the number of elements in the symmetric difference $S_i \Delta S_j = (S_i \setminus S_j) \cup (S_j \setminus S_i)$. Let \mathfrak{S}_0^M be the multi-set form of \mathfrak{S}_0 , so that S_i is appeared $r(S_i)$ times in \mathfrak{S}_0^M . As an example, for $\mathfrak{S}_0 = \{(\{1, 2, 3\}, 2), (\{1, 2\}, 1)\}$, $\mathfrak{S}_0^M = \{\{1, 2, 3\}, \{1, 2, 3\}, \{1, 2\}\}$. Then,

$$\text{diff}(\mathfrak{S}_{0,1}, \mathfrak{S}_{0,2}) := \sum_{S \in \mathfrak{S}_{2 \setminus 1}} \min_{S' \in \mathfrak{S}_{1 \setminus 2}} d_p(S, S')^2 + \sum_{S \in \mathfrak{S}_{1 \setminus 2}} \min_{S' \in \mathfrak{S}_{2 \setminus 1}} d_p(S, S')^2,$$

where $\mathfrak{S}_{2 \setminus 1} = \mathfrak{S}_{0,2}^M \setminus \mathfrak{S}_{0,1}^M$ and $\mathfrak{S}_{1 \setminus 2} = \mathfrak{S}_{0,1}^M \setminus \mathfrak{S}_{0,2}^M$. See Section B.1 of the supplementary material for examples and rationale for using diff.

4. Theory

Given an ordering of index-sets in $(2^{\mathcal{K}} \setminus \{\phi\}, \subset)$ and the signal blocks $Z = \{Z_k : k \in \mathcal{K}\}$, the partially-joint structure $\mathfrak{S}(Z) = \{(S_i, r(S_i), W_i) : i \in \mathcal{I}_K\}$ is uniquely determined. Unfortunately, for different orderings of $(2^{\mathcal{K}} \setminus \{\phi\}, \subset)$, the ranks $r(S_i)$ and the partially-joint score subspaces $[W_i]$ may be different. In this section, we introduce conditions on relations among $[V_k]$'s for $\mathfrak{S}(Z)$ to be uniquely determined regardless of the choice of the orders of $(2^{\mathcal{K}} \setminus \{\phi\}, \subset)$.

For each $l = 1, \dots, K$, let $\mathcal{J}_l = \{i \in \mathcal{I}_K : |S_i| = l\}$ be the set of all indices with size l . For $l = 1, \dots, K - 1$, we set $[I_l] = +_{i \in \{i: |S_i| > l\}} (\cap_{k \in S_i} [V_k]) = +_{i \in \{i: |S_i| > l\}} [W_i]$, and the projection onto $[I_l]^\perp$ in \mathbb{R}^n is denoted by $P_{I_l}^\perp$. Note that when evaluating the rank for $[W_i]$ for $i \in \mathcal{J}_l$, the definition of $[W_i]$ in (4) utilizes the deflated score subspaces orthogonal to $[I_l]$, using the given order of S_i 's among $i \in \mathcal{J}_l$. We say $\{[V_k]\}_{k \in \mathcal{K}}$ to be *relatively independent* if, for every $l = 1, \dots, K - 1$ and $i \in \mathcal{J}_l$, $P_{I_l}^\perp(\cap_{k \in S_i} [V_k])$ is linearly independent to $[C_{l,-i}] = +_{j \in \mathcal{J}_l \setminus \{i\}} (P_{I_l}^\perp(\cap_{k \in S_i} [V_k]))$. In words, $\{[V_k]\}_{k \in \mathcal{K}}$ is relatively independent, if for each and every layer \mathcal{J}_l , each deflated subspace is linearly independent to $[C_{l,-i}]$, the sum of the other deflated subspaces in the layer \mathcal{J}_l . If $P_{I_l}^\perp(\cap_{k \in S_i} [V_k])$ is orthogonal to $[C_{l,-i}]$ for every $l = 1, \dots, K - 1$ and $i \in \mathcal{J}_l$, then $\{[V_k]\}_{k \in \mathcal{K}}$ is said to be *relatively orthogonal*. We immediately check that relative orthogonality implies relative independence.

Theorem 1. *Given matched data matrices $X_k = Z_k + E_k \in \mathbb{R}^{p_k \times n}$ for $k = 1, \dots, K$ with true signal Z_k and error E_k , if $\{[V_k]\}_{k \in \mathcal{K}}$, the collection of Z_k 's signal score subspaces, is relatively independent, then, regardless of the ordering of index-sets in $(2^{\mathcal{K}} \setminus \{\phi\}, \subset)$, there exists a unique set of pairs $\{(S_i, r(S_i))\}_{i \in \mathcal{I}_K}$.*

Under only the relative independence condition, the determination of the partially-joint score subspaces $[W_i]$ corresponding to S_i , $i \in \mathcal{I}_K$, may not be unique, and depends on the ordering of index-sets (see Examples A.3 and A.4 in the supplementary material). To ensure uniqueness of $[W_i]$'s, we require a rather strong assumption. We say that $\{[V_k]\}_{k \in \mathcal{K}}$ is *absolutely orthogonal*, if (1) $\{[V_k]\}_{k \in \mathcal{K}}$ satisfies relative orthogonality, and (2) for each $l = 1, \dots, K - 1$

and for every $i \in \mathcal{I}_l$,

$$P_{I_l}^\perp(\cap_{k \in S_i} [V_k]) = P_{J_i}^\perp(\cap_{k \in S_i} [V_k]), \quad (14)$$

where $[J_i] = +_{j \in \mathcal{J}_{i,>l}}(\cap_{k \in S_j} [V_k]) = +_{j \in \mathcal{J}_{i,>l}} [W_j]$ and $\mathcal{J}_{i,>l} = \{j : |S_j| > l, S_i \cap S_k \neq \emptyset\}$. In Example 2.1, when $l = 1$ and $i = 6$, (14) holds if $(\bigcirc_{j \in \{1,2,3,4\}} P_j^\perp)([V_1]) = (\bigcirc_{j \in \{1,2,3\}} P_j^\perp)([V_2])$. Note that for $i = 6$, $S_i = \{2\}$ and the index-sets S_j 's for $j \in \mathcal{J}_{i,>l}$ are $S_1 = \{1, 2, 3\}$, $S_2 = \{1, 2\}$, $S_3 = \{2, 3\}$, excluding $S_4 = \{1, 3\}$.

Theorem 2. *Given matched data matrices $X_k = Z_k + E_k \in \mathbb{R}^{p_k \times n}$ for $k = 1, \dots, K$ with true signal Z_k and error E_k , if $\{[V_k]\}_{k \in \mathcal{K}}$ is absolutely orthogonal, then partially-joint score subspaces $[W_i]$ for $i \in \mathcal{I}_K$ are uniquely determined.*

The uniqueness of each partially-joint loading subspace $[U_{(k),i}]$ is deduced from the uniqueness of $[W_i]$'s.

Corollary 1. *Given matched data matrices $X_k = Z_k + E_k \in \mathbb{R}^{p_k \times n}$ for $k = 1, \dots, K$ with true signal Z_k and error E_k , if $\{[V_k]\}_{k \in \mathcal{K}}$ is absolutely orthogonal, then each partially-joint loading subspace $[U_{(k),i}]$ is uniquely determined for $k = 1, \dots, K$ and $i \in \mathcal{I}_{(k)}$.*

We provide proofs of theorems in this section and examples for relative independence and absolute orthogonality in Section A of the supplementary material.

5. Simulation Study

5.1. Example Dataset Generation

In the simulation study, we use the following data generation setting for numerically analyzing the performance of our proposal. Throughout, we use $K = 3$ blocks of data sets, in which the association structures are given by the ranks of index-sets.

First, we set a pre-determined rank $r(S_i)$ for each index-set S_i for $i = 1, \dots, 2^K - 1$. The generic partially-joint score matrix $W_{comp,i} \in \mathbb{R}^{n \times r(S_i)}$ for each index-set is a column-wise concatenation of randomly generated vectors $w_{comp,i,j}$ for $j = 1, \dots, r(S_i)$. Each $w_{comp,i,j}$ are generated element-wise and the entries of $w_{comp,i,j}$ follows $\mathcal{N}(0, \sigma_{i,j}^2)$ independently; not only independent within a $w_{comp,i,j}$, but independent between $w_{comp,i,j}$'s as well. The magnitude

of signal $\sigma_{i,j}^2$'s depends on the simulation settings, and summarized as $\sigma_M^2 = \{(\sigma_{i,j}^2) : i \in \mathcal{I}_K, j = 1, \dots, r(S_i), r(S_i) > 0\}$. The column-wise concatenation of $W_{comp,i}$ is denoted W_{comp} of size $n \times \sum_{i=1}^{2^K-1} r(S_i)$.

The generic loading matrices $U_{comp,k,i} \in \mathbb{R}^{p_k \times r(S_i)}$ for $i = 1, \dots, 2^K - 1$ and $k = 1, \dots, K$ are given as follows. The entries of $U_{comp,k,i}$ are generated independently from the uniform distribution, $\text{Unif}(0, 1)$, and all the columns of $U_{comp,k,i}$ are scaled. We give $U_{comp,k,i}$ orthonormality by the QR decomposition. We then derive the generic signal matrix Z_k for $k = 1 \dots, K$ by $Z_k = \text{weight}_k \cdot \sum_{i=1}^{2^K-1} (U_{comp,k,i} \cdot W_{comp,i})$, where weight_k 's are weights for each dataset, which reflect the magnitude of signals. The concatenation of generic loading matrices is denoted U_{comp} , and is of size $\sum_{k=1}^K p_k \times \sum_{i=1}^{2^K-1} r(S_i)$.

The error matrix E_k is generated element-wisely, such that $e_{k,ij} \sim \mathcal{N}(0, \sigma^2)$ independently for $i = 1, \dots, p_k$ and $j = 1, \dots, n$. The magnitude of error σ^2 is set as the reciprocal of the signal-to-noise ratio (SNR), $\sigma^2 = 1/\text{SNR}$, where SNR is predetermined as a simulation setting.

We use the following six models. We set $n = 200$, $p_1 = p_2 = p_3 = 100$ and $\text{weight}_1 = \text{weight}_2 = \text{weight}_3 = 1$, for all six cases. Recall that the *partially-joint structure* is summarized by $\mathfrak{S}_0 = \{(S_i, r(S_i)) : i \in \mathcal{I}_K, r(S_i) > 0\}$.

1. (Individuals) $\mathfrak{S}_0 = \{(\{1\}, 2), (\{2\}, 2), (\{3\}, 2)\}$, $\sigma_M^2 = \{(1.4, 0.8), (1.3, 0.7), (1.2, 0.6)\}$
2. (Fully joint) $\mathfrak{S}_0 = \{(\{1, 2, 3\}, 2)\}$, $\sigma_M^2 = \{(1.0, 0.9)\}$
3. (Circular, partially joint) $\mathfrak{S}_0 = \{(\{1, 2\}, 2), (\{1, 2\}, 2), (\{1, 3\}, 2)\}$, $\sigma_M^2 = \{(1.4, 0.8), (1.3, 0.7), (1.2, 0.6)\}$
4. (Mix of fully joint and individuals) $\mathfrak{S}_0 = \{(\{1, 2, 3\}, 2), (\{1\}, 2), (\{2\}, 2), (\{3\}, 2)\}$, $\sigma_M^2 = \{(1.5, 0.8), (1.4, 0.7), (1.3, 0.6), (1.2, 0.5)\}$
5. (Fully joint and partially joint) $\mathfrak{S}_0 = \{(\{1, 2, 3\}, 2), (\{1, 2\}, 2), (\{1, 3\}, 2), (\{2, 3\}, 2)\}$, $\sigma_M^2 = \{(1.5, 0.8), (1.4, 0.7), (1.3, 0.6), (1.2, 0.5)\}$
6. (All possible combinations) $\mathfrak{S}_0 = \{(\{1, 2, 3\}, 2), (\{1, 2\}, 2), (\{1, 3\}, 2), (\{2, 3\}, 2), (\{1\}, 2), (\{2\}, 2), (\{3\}, 2)\}$, $\sigma_M^2 = \{(1.8, 0.8), (1.7, 0.7), (1.6, 0.6), (1.5, 0.5), (1.4, 0.4), (1.3, 0.3), (1.2, 0.2)\}$

For each multi-block data set, we first determine the signal rank r_k for each dataset X_k , using `getnfac` function of R package `PANICr` with option `IC3` (Bai and Ng, 2002).

5.2. Results on Comparative Study

In this subsection, we numerically compare the performance of our proposal to other competitors, including SLIDE (Gaynanova and Li, 2019), COBS (Gao et al., 2021), AJIVE (Feng et al., 2018), and JIVE (Lock et al., 2013). Note that from the estimates of each method, the partially-joint structure \mathfrak{S} can be extracted, as well as the concatenated partially-joint score matrix \widehat{W} and loading matrix \widehat{U} . See Section B.2 of the supplementary material for a brief review of these methods. Our proposal will be called the method of partially-joint structure identification, or PSI for short.

To assess the efficacy of finding the true partially-joint structure $\widehat{\mathfrak{S}}_0$ and proper loading and score matrices, we use the following measures.

- (1) *Partially-joint structure $\widehat{\mathfrak{S}}_0$* : The rate of finding the true partially-joint structure, $\mathbb{E}\mathbb{1}(\mathfrak{S}_0 = \widehat{\mathfrak{S}}_0)$.
- (2) *Partially-joint loading matrix \widehat{U}* : We find the difference between U_{comp} and \widehat{U} as follows. We denote the principal angles between $U_{comp,k,i}$ and $\widehat{U}_{(k)}$ by $\theta_{U,k,i,j}$ for $k = 1, \dots, K$, $i = 1, \dots, 2^K - 1$ and $j = 1, \dots, r(S_i)$. We report the average of all the values of $\theta_{U,k,i,j}$'s as $\bar{\theta}(U, \widehat{U})$.
- (3) *Partially-joint score matrix \widehat{W}* : We find the difference between W_{comp} and \widehat{W} as follows. We denote the principal angle between $w_{comp,i,j}$ and \widehat{W} by $\theta_{W,i,j}$ for $i = 1, \dots, 2^K - 1$ and $j = 1, \dots, r(S_i)$. We report the average of all the values of $\theta_{W,i,j}$'s as $\bar{\theta}(W, \widehat{W})$.

In the comparative study, the measures $\mathbb{E}\mathbb{1}(\mathfrak{S}_0 = \widehat{\mathfrak{S}}_0)$, $\bar{\theta}(U, \widehat{U})$ and $\bar{\theta}(W, \widehat{W})$ were computed to assess the performance of PSI and other four methods. The simulation was conducted on different values of SNR (10 and 5) for the example models 1 to 6. Given a fixed true partially-joint loading matrix U_{comp} , one hundred data sets were generated for each SNR value. We tested all 5 methods over these datasets. Average and standard deviation for each measure are reported in Tables 1 and 2.

In the example model 1, in which case there are only individual scores, PSI and AJIVE identified the true partially-joint structure for almost all instances. In the example model 2, in which case there are only joint score, all methods but JIVE find the true structure for almost all SNRs and instances. PSI and AJIVE have estimated identical score subspaces, but our

Table 1: Comparative Study on Model 1 to 3. The unit for $\mathbb{E}\mathbb{1}(\mathfrak{S}_0 = \widehat{\mathfrak{S}}_0)$ is percent.

Model	SNR	Measure	PSI	SLIDE bcv	COBS	AJIVE	JIVE
1	10	$\mathbb{E}\mathbb{1}(\mathfrak{S}_0 = \widehat{\mathfrak{S}}_0)$	100 (0)	2 (14.07)	17 (37.75)	95 (21.9)	93 (25.64)
		$\bar{\theta}(U, \widehat{U})$	13.78 (0.53)	25.58 (12.48)	50.43 (10.05)	14.07 (1.86)	13.9 (0.56)
		$\bar{\theta}(W, \widehat{W})$	18.52 (0.59)	19.57 (0.72)	20.87 (1.16)	18.53 (0.55)	18.89 (0.58)
	5	$\mathbb{E}\mathbb{1}(\mathfrak{S}_0 = \widehat{\mathfrak{S}}_0)$	99 (10)	5 (21.9)	45 (50)	96 (19.69)	83 (37.75)
		$\bar{\theta}(U, \widehat{U})$	20.22 (0.87)	37.48 (16.37)	67.2 (6.57)	20.82 (3.37)	20.42 (0.87)
		$\bar{\theta}(W, \widehat{W})$	26.21 (1.17)	28.83 (3.2)	35.07 (3.63)	26.35 (1.77)	26.38 (0.84)
2	10	$\mathbb{E}\mathbb{1}(\mathfrak{S}_0 = \widehat{\mathfrak{S}}_0)$	100 (0)	100 (0)	100 (0)	100 (0)	62 (48.78)
		$\bar{\theta}(U, \widehat{U})$	13.01 (0.54)	13.04 (0.54)	19.39 (1.72)	60.44 (0.43)	13.05 (0.55)
		$\bar{\theta}(W, \widehat{W})$	10.95 (0.56)	11.52 (0.92)	11.26 (0.62)	10.95 (0.56)	11.5 (0.95)
	5	$\mathbb{E}\mathbb{1}(\mathfrak{S}_0 = \widehat{\mathfrak{S}}_0)$	100 (0)	100 (0)	100 (0)	100 (0)	58 (49.6)
		$\bar{\theta}(U, \widehat{U})$	18.46 (0.8)	18.49 (0.8)	32.37 (3.02)	62.2 (0.59)	18.49 (0.81)
		$\bar{\theta}(W, \widehat{W})$	15.82 (0.85)	16.11 (1.02)	17.28 (1.14)	15.82 (0.85)	16.07 (1.04)
3	10	$\mathbb{E}\mathbb{1}(\mathfrak{S}_0 = \widehat{\mathfrak{S}}_0)$	100 (0)	17 (37.75)	2 (14.07)	0 (0)	0 (0)
		$\bar{\theta}(U, \widehat{U})$	13.29 (0.4)	24.44 (8.74)	26.97 (5.51)	39.09 (3.61)	15.11 (2.52)
		$\bar{\theta}(W, \widehat{W})$	13.31 (0.41)	13.87 (0.52)	14.52 (0.63)	13.71 (0.78)	14.17 (0.81)
	5	$\mathbb{E}\mathbb{1}(\mathfrak{S}_0 = \widehat{\mathfrak{S}}_0)$	78 (41.63)	45 (50)	9 (28.76)	0 (0)	0 (0)
		$\bar{\theta}(U, \widehat{U})$	19.20 (0.77)	33.33 (7.8)	47.61 (6.63)	47.15 (2.91)	20.89 (2.42)
		$\bar{\theta}(W, \widehat{W})$	19.17 (0.64)	19.52 (0.7)	26.13 (2.7)	20.63 (1.29)	19.89 (1.09)

method performs better in estimating loading subspaces. This is because PSI estimates the loading spaces as $\widehat{U}_k = \widehat{Z}_k \widehat{W}$, compared to AJIVE with $\widehat{U}_k = X_k \widehat{W}$, so PSI can avoid noise in computation. In the example model 3, in which partially-joint scores are entangled in a cyclic structure, PSI boasts superior performances in identifying the true structures. Table 1 confirms these observations.

In the example model 4, in which case both joint and individual scores are composited, both PSI and AJIVE showed superior performance in identifying the true structure. Our method was as competent in estimating score subspaces as AJIVE. In the example model 5 and 6, the complicated cases with joint, partially-joint and individual scores mixed, PSI is prominent in estimating true structure, loading and score subspaces. See Table 2.

Our method took remarkably less computation time in almost all situations. PSI took 0.79 to 2.88 seconds in computation, compared to the time ranges from 0.87 to 22.82 seconds for SLIDE, and from 3.85 to 27.61 seconds for COBS. AJIVE took about 11 seconds consistently for all cases. JIVE exhibits the longest computation times. Table B.1 in the supplementary materials shows time comparison between our methods and other four methods.

Table 2: Comparative Study on Model 4 to 6. The unit for $\mathbb{E}\mathbb{1}(\mathfrak{S}_0 = \widehat{\mathfrak{S}}_0)$ is percent.

Model	SNR	Measure	PSI	SLIDE bcv	COBS	AJIVE	JIVE
4	10	$\mathbb{E}\mathbb{1}(\mathfrak{S}_0 = \widehat{\mathfrak{S}}_0)$	100 (0)	1 (10)	19 (39.43)	100 (0)	82 (38.61)
		$\bar{\theta}(U, \widehat{U})$	13.33 (0.39)	18.6 (0.4)	35.37 (4.76)	37.59 (0.36)	13.52 (1.01)
		$\bar{\theta}(W, \widehat{W})$	17.03 (0.47)	18.03 (0.61)	19.28 (1.16)	16.99 (0.47)	17.45 (0.53)
	5	$\mathbb{E}\mathbb{1}(\mathfrak{S}_0 = \widehat{\mathfrak{S}}_0)$	92 (27.27)	4 (19.69)	28 (45.13)	100 (0)	53 (50.16)
		$\bar{\theta}(U, \widehat{U})$	19.65 (1.25)	29.33 (9.48)	47.92 (2.13)	41.62 (0.55)	19.51 (1.05)
		$\bar{\theta}(W, \widehat{W})$	24.37 (1.56)	28.22 (4.78)	32.84 (2.79)	24.06 (0.74)	24.32 (0.75)
5	10	$\mathbb{E}\mathbb{1}(\mathfrak{S}_0 = \widehat{\mathfrak{S}}_0)$	100 (0)	30 (46.06)	0 (0)	0 (0)	0 (0)
		$\bar{\theta}(U, \widehat{U})$	13.33 (0.38)	22.04 (6.02)	24.51 (2.22)	44.42 (2.16)	16.98 (1.39)
		$\bar{\theta}(W, \widehat{W})$	13.00 (0.34)	13.57 (0.45)	14.24 (0.52)	13.28 (0.55)	14.24 (0.53)
	5	$\mathbb{E}\mathbb{1}(\mathfrak{S}_0 = \widehat{\mathfrak{S}}_0)$	69 (46.48)	60 (49.24)	0 (0)	0 (0)	0 (0)
		$\bar{\theta}(U, \widehat{U})$	19.86 (1.85)	29.73 (5.56)	42.45 (4.34)	50.22 (1.76)	21.98 (1.45)
		$\bar{\theta}(W, \widehat{W})$	18.98 (0.85)	19.04 (0.59)	25.46 (2.18)	19.75 (0.93)	19.37 (0.77)
6	10	$\mathbb{E}\mathbb{1}(\mathfrak{S}_0 = \widehat{\mathfrak{S}}_0)$	5 (21.9)	0 (0)	0 (0)	0 (0)	0 (0)
		$\bar{\theta}(U, \widehat{U})$	16.61 (1.06)	29.92 (10.51)	32.72 (2.56)	44.1 (1.28)	18.42 (1.19)
		$\bar{\theta}(W, \widehat{W})$	20.17 (1.32)	20.27 (2.21)	24.28 (1.22)	17.47 (0.57)	18.33 (0.47)
	5	$\mathbb{E}\mathbb{1}(\mathfrak{S}_0 = \widehat{\mathfrak{S}}_0)$	0 (0)	0 (0)	0 (0)	0 (0)	0 (0)
		$\bar{\theta}(U, \widehat{U})$	27.18 (3.59)	32.42 (9.97)	46.54 (3.03)	46.13 (1.6)	24.63 (1.33)
		$\bar{\theta}(W, \widehat{W})$	30.25 (2.36)	28.25 (1.36)	33.78 (0.97)	25.62 (0.98)	25.66 (0.84)

5.3. Results on Imbalanced Signal Strength between Joint and Individual Components

Next, we consider cases where the signal strengths of joint components and individual components are grossly imbalanced. Consider a new model, with $K = 3$ and $p_1 = p_2 = p_3 = 100$, whose index-set ordering is $S_1 = \{1, 2, 3\}$, $S_5 = \{1\}$, $S_6 = \{2\}$ and $S_7 = \{3\}$. We set inherent joint rank $r(S_1) = 10$ and individual ranks $r(S_5) = r(S_6) = r(S_7) = 10$. Other index-sets have zero ranks, $r(S_2) = r(S_3) = r(S_4) = 0$. Throughout, $n = 200$.

For the case in which there are larger variations in the joint component than the individual components, we set $\sigma_{1,j}^2 \gg \sigma_{i,j}^2$ for $i = 5, 6, 7$ and all j 's. In the opposite case, we give larger variations in the individual components than the joint component, $\sigma_{i,j}^2 \gg \sigma_{1,j}^2$ for $i = 5, 6, 7$ and all j 's. Details are given in Section B.5 of the supplementary materials.

We carried out comparative simulations on both cases at SNR levels ∞ and 5. Not only the success rate of finding true structure but also the numbers of estimated joint and individual components were evaluated. In Table 3, in which case the joint component has larger variations, JIVE showed superior performances to other methods, but PSI is also compatible in identifying joint and individual components. PSI did not succeed in identifying individual components for SNR = 5, because initial rank estimations failed to distinguish the weak individual signals from noise. When the individual components have larger variations, in Table 4, our method shows more

Table 3: The case where the joint component has larger variations than the individual components.

SNR	Measure	PSI	SLIDE bcv	COBS	AJIVE	JIVE
∞	$\mathbb{E}l(\mathfrak{S}_0 = \widehat{\mathfrak{S}}_0)$	31 (46)	0 (0)	0 (0)	0 (0)	92 (27.27)
	Joint	10 (0)	10 (0)	39.46 (0.82)	4 (2.01)	9.92 (0.27)
	Individual	32.3 (2.56)	0 (0)	0.04 (0.24)	48 (6.02)	27.84 (7.36)
5	$\mathbb{E}l(\mathfrak{S}_0 = \widehat{\mathfrak{S}}_0)$	0 (0)	0 (0)	0 (0)	0 (0)	4 (19.69)
	Joint	10 (0)	10 (0)	13.08 (1.67)	10 (0)	9.92 (0.27)
	Individual	0 (0)	0 (0)	17.98 (2.6)	32.53 (0.9)	32.05 (10.27)

Table 4: The case where the individual components have larger variations than the joint components.

SNR	Measure	PSI-MDI	SLIDE bcv	COBS	AJIVE	JIVE
∞	$\mathbb{E}l(\mathfrak{S}_0 = \widehat{\mathfrak{S}}_0)$	78 (41.63)	0 (0)	0 (0)	0 (0)	0 (0)
	Joint	10 (0)	0.23 (0.47)	38.86 (1.11)	3.94 (1.73)	3.46 (1.38)
	Individual	30.4 (0.89)	26.86 (1.14)	0.05 (0.26)	48.18 (5.2)	27.82 (1.31)
5	$\mathbb{E}l(\mathfrak{S}_0 = \widehat{\mathfrak{S}}_0)$	0 (0)	0 (0)	0 (0)	0 (0)	0 (0)
	Joint	6.05 (1.73)	0.68 (0.68)	31.26 (2.75)	0.92 (0.54)	2.88 (1.21)
	Individual	35.09 (3.45)	28.93 (1.77)	2.73 (1.51)	57.26 (1.64)	27.91 (1.32)

robust performances in finding both joint and individual components than other methods.

6. Real Data Analysis

In this section, we apply the proposed PSI to a dataset called EGAS0000100174, a blood cancer multi-omics data set linked to a drug response panel (Dietrich et al., 2018). We have chosen to use 121 cases diagnosed with chronic lymphocytic leukemia (CLL). The drug response panel (X_{Drug}) records the *ex vivo* cell viabilities at a series of 5 concentrations, for each of 62 drugs that target onco-related pathways or are used widely in clinical practice. This multi-omics data set consists of the genome-wide DNA methylation profiles and the RNA sequencing profiles. The top 5,000 most variable CpG sites were selected (X_{Meth}) from the *450K illumina assay* DNA methylation profile. As for the RNA sequencing profile, we selected the top 5,000 gene expressions with the largest stabilized variances (X_{Exp}) from the high-throughput sequencing (HTS) assay. In summary, we have three blocks of data sets $X_{\text{Drug}} \in \mathbb{R}^{121 \times 310}$, $X_{\text{Meth}} \in \mathbb{R}^{121 \times 5000}$ and $X_{\text{Exp}} \in \mathbb{R}^{121 \times 5000}$.

We repeat the estimation process over 100 repetitions (of data splitting) and select the mode structure, that is, the estimated partially-joint structure that appears the most out of 100 repetitions. The estimated mode structure

is

$$\widehat{\mathfrak{S}}_0 = \{(\{\text{Drug, Meth}\}, 1), (\{\text{Drug}\}, 4), (\{\text{Meth}\}, 41), (\{\text{Exp}\}, 3)\},$$

which means that PSI detected the index-set $\{\text{Drug, Meth}\}$ of rank 1, and no fully-joint score or other forms of partially-joint scores were detected. This structure appeared 53 times out of 100 repetitions. The index-set $\{\text{Drug, Meth}\}$ of rank 1 stands for the existence of one-dimensional latent score, partially-joint for Drug and Meth data sets (but not for Exp data set).

PSI showed better performance in computation time over other methods. In an Intel[®] Xeon[®] CPU E5-2640 v4 @ 2.40GHz system, it took 9.38 seconds per single data splitting instance (54.56 seconds for 100 instances with 40 cores). In comparison, the SLIDE with bcr method detected the same structure as our method, but it took almost 9 hours on the same machine. The COBS yielded an eccentric result, giving the fully-joint score of rank 50, taking about 14 minutes.

PSI was also robust over different choices of initial ranks. As a preprocessing, we set the ranks of the signal matrices using the principal component analysis which accounts for cumulative proportion of variances at 30%, 40%, 50% and 60%. Resulting signal ranks for Drug, Meth and Exp datasets are (2, 6, 1), (2, 15, 1), (3, 28, 2) and (5, 42, 3), respectively. For all cases, PSI detected the same index-set $\{\text{Drug, Meth}\}$ of rank 1.

The analysis by PSI for the patient sample multi-block data reveals a particular pattern in the latent partially-joint score, which cannot be identified by applying, e.g. principal component analysis to each data block. To support this claim, we plot the reconstructed matrices $\widehat{U}_{(k),i}\widehat{W}_i^T$ for the identified partially-joint and individual parts of the data in Fig. 3. Both the samples and the variables of X_{Drug} are ordered by a hierarchical bi-clustering applied to the partially-joint component $\widehat{U}_{(\text{Drug}),2}\widehat{W}_2^T$ of X_{Drug} , where $\widehat{W}_2 = \widehat{W}_{\{\text{Drug, Meth}\}}$. The matrix $Z_{\text{Drug},S_2} := \widehat{U}_{(\text{Drug}),2}\widehat{W}_2^T$ is shown in the top left part of Fig. 3. The variables of X_{Meth} are similarly ordered.

Focusing on the partially-joint scores corresponding to $\{\text{Drug, Meth}\}$, the samples are clustered into two distinct subgroups. These subgroups are shown in Fig. 4(a), and are denoted by groups α and β . There, it can be seen that the variables in X_{Drug} and X_{Meth} show a contrasting pattern according to the two subgroups α and β . Comparing Z_{Drug,S_2} (Fig. 4(a)) with the whole X_{Drug} (Fig. 4(b)), we observe that the subgroups identified above are hidden in X_{Drug} . Moreover, the subgroups α and β are well-separated in the

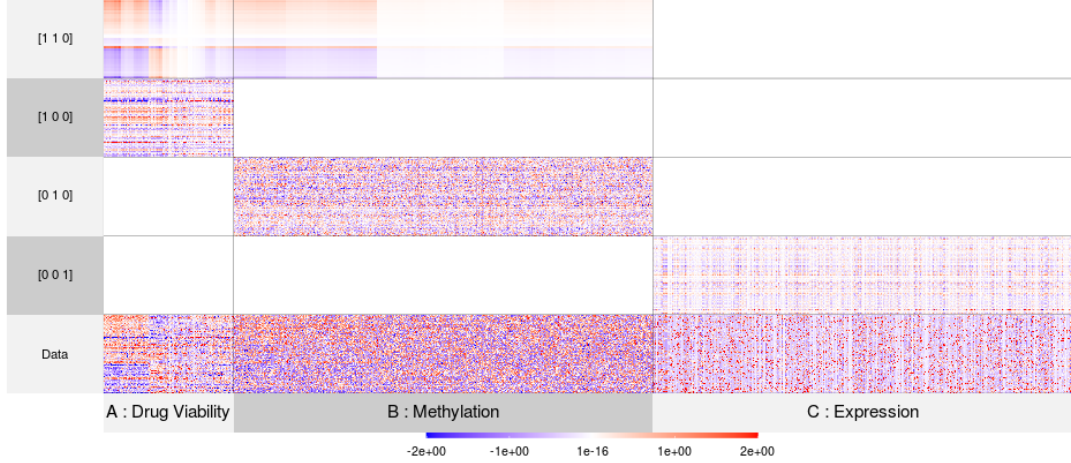


Figure 3: The reconstructed components according to the estimated partially-joint structure. The values are all normalized for each column, then truncated to line on $[-2, 2]$.

partially-joint score $\widehat{W}_{\{\text{Drug}, \text{Meth}\}}$ of Z_{Drug, S_2} (Fig. 4(c)), while it is hard to find any subgroup in the principal component scores of whole X_{Drug} (Fig. 4(d)). The same conclusion can be made by inspecting the component of X_{Meth} corresponding to the partially-joint score $\widehat{W}_{\{\text{Drug}, \text{Meth}\}}$, denoted Z_{Meth, S_2} , and the whole X_{meth} in Fig. 4(e) and (f). Thus we observed that PSI gives a more effective measure of finding inherent subgroups in a multi-omics data set than a separate application of the principal component analysis on each of the data matrix.

To find indicators that best explain the subgroups α and β , we conducted the Fisher exact test simultaneously on 59 gene mutations or chromosome defects of each patients, available as an ancillary information. The p-values from each Fisher exact test were adjusted by the Benjamini-Hochberg (BH) method. The smaller p-values indicate stronger differences of each mutation or chromosome defect between the subgroup α and β . We found that the immunoglobulin heavy chain variable (IGHV) region mutation status has the most associated relation with the subgroups at BH-adjusted p-value 1.026×10^{-13} . We also present the 2×2 table of the IGHV status and the subgroups, see Tables C.1 and C.2 in the supplementary material. We postulate

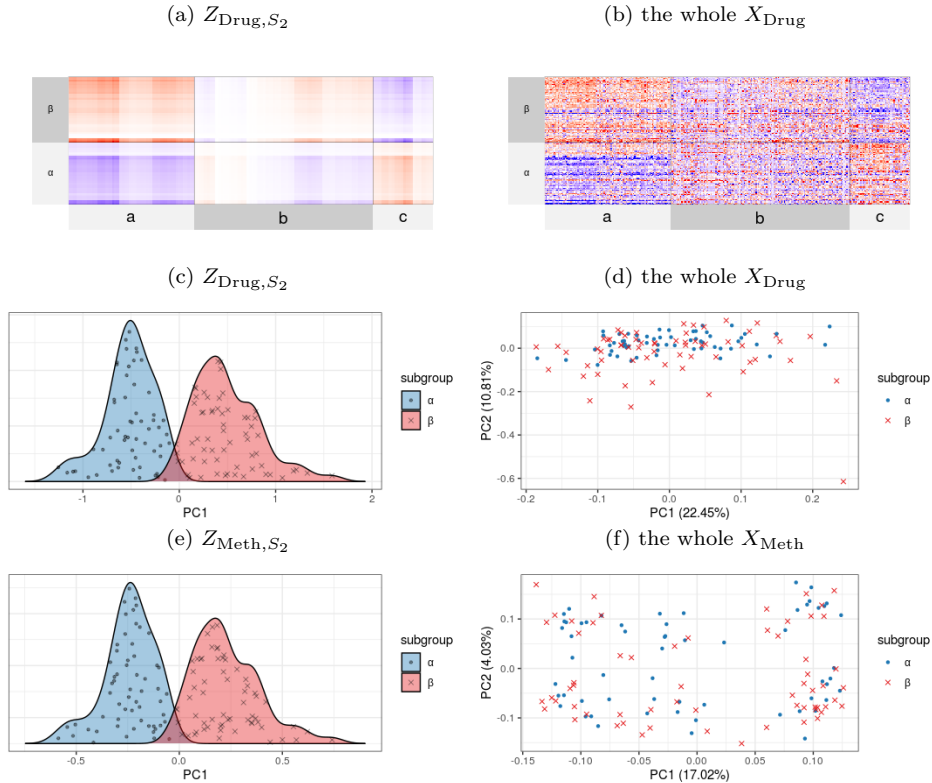


Figure 4: (a) The matrix $Z_{\text{Drug},S_2} := \widehat{U}_{(\text{Drug}),2} \widehat{W}_2^T$. (b) The whole X_{Drug} data matrix. (c) The density plot of the subgroups α and β along the first principal component (PC) score of Z_{Drug,S_2} ; (d) The PC scores plot for the whole X_{Drug} ; (e) The density plot of the subgroups α and β along the first principal component of Z_{Meth,S_2} ; (f) The PC scores plot of the whole X_{Meth} .

IGHV mutation status gives a substantial explanation for the subgrouping of CLL patients, that is, wild type matches to the subgroup α and mutation type to the subgroup β . Survival analyses on overall survival rates was also conducted, and we found statistically significant differences in survival between the two subgroups α and β as shown in Fig. 5.

Again in Fig. 4(a), the variables in Z_{Drug,S_2} can be clustered into subgroups [a] and [b] showing a contrasting response pattern to the subgroups α and β (variables showing weak responses were excluded as subgroup [c]). The subgroup [a] shows higher viability for β (IGHV mutated) than α (IGHV wild type) and vice versa for [b]. Table C.3 (in the supplementary material) presents the list of prominent drugs that have appeared in subgroups [a] and

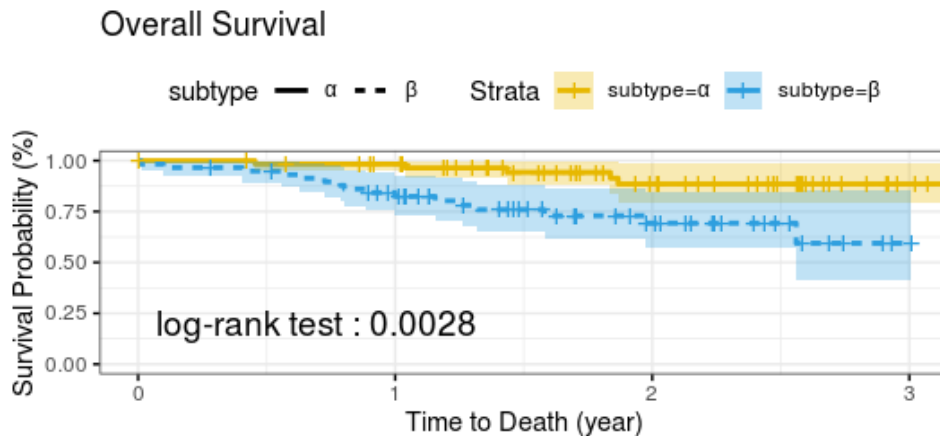


Figure 5: The difference in overall survival between the subgroups α and β is displayed on a Kaplan plot with p-value 0.0028 from the log-rank test.

[b] at least 4 times out of 5 concentrations. For the subgroup [a], the table lists a number of inhibitor drugs that target the B cell receptor (BCR) components, such as Bruton’s tyrosine kinase (BTK; spebrutinib, ibrutinib), phosphatidylinositol 3-kinase (PI3K; idelalisib, duvelisib) and spleen tyrosine kinase (STK; tamatinib, PRT062607 HCL). AKT inhibitor(MK-2206) or SRC inhibitors (dasatinib) targets signal transduction pathways that promotes survival and growth of B cell lymphocytes. Unexpected encounter with HSP90 inhibitor (AT13387 or Onalespib) may be related to the stability of lymphocyte-specific SRC family kinases (Mshaik et al., 2021). The appearance of CHK inhibitors (PF 477736, AZD7762, CCT241533) may be linked to repairing mechanisms of DNA damages at G2 phase, known to be associated with WEE1 kinase and the AKT/PKB pathway (Zhang and Hunter, 2014). For the subgroup [b], the appearance of mTOR inhibitor (everolimus) may suggest that mTOR pathway and shows different drug sensitivities to the BCR component, despite the fact that it is on the downstream of AKR/PKB pathway. The role of IGHV in this implication requires further investigation. BCL2 inhibitor (navitoclax) and rotenone might be related to the role of mitochondria in apoptosis (Wang and Youle, 2014).

Supplementary Materials

The supplementary materials contain the proofs of Lemma 2.1, Theorems 1 and 2 and Corollary 1, a brief review on competing methods, detailed model settings used for simulations, additional numerical results and auxiliary information on real data analysis, including the table of drugs selected by the proposed method.

References

- Bai, J., Ng, S., 2002. Determining the number of factors in approximate factor models. *Econometrica* 70(1), 191–221.
- Björck, A., Golub, G., 1973. Numerical methods for computing angles between linear subspaces. *Mathematics of Computation* 27(123), 579–594.
- Dietrich, S., Oleś, M., Lu, J., Sellner, L., et al., 2018. Drug-perturbation-based stratification of blood cancer. *Journal of Clinical Investigation* 128(1), 427–445.
- Draper, B., Kirvy, M., Marks, J., Marrinan, T., Peterson, C., 2014. A flag representation for finite collections of subspaces of mixed dimensions. *Linear Algebra and its Applications* 451, 15–32.
- Eckart, C., Young, G., 1936. The approximation of one matrix by another of lower rank. *Psychometrika* 1, 211–218.
- Feng, Q., Jiang, M., Hannig, J., Marron, J., 2018. Angle-based joint and individual variation explained. *Journal of Multivariate Analysis* , 241–265.
- Gao, X., Lee, S., Jung, S., 2021. Covariate-driven factorization by thresholding for multi-block data. *Biometrics* 77(3), 1011–1023.
- Gaynanova, I., Li, G., 2019. Structural learning and integrative decomposition of multi-view data. *Biometrics* 75, 1121–1132.
- Jung, S., Lee, M.H., Ahn, J., 2018. On the number of principal components in high dimensions. *Biometrika* 105(2), 389–402.
- Li, G., Gaynanova, I., 2018. A general framework for association analysis of heterogeneous data. *The Annals of Applied Statistics* 12(3), 1700–1726.

- Li, G., Jung, S., 2017. Incorporating covariates into integrated factor analysis of multi-view data. *Biometrics* 72, 1433–1442.
- Lock, E., Hoadley, K., Marron, J., Nobel, A., 2013. Joint and individual variation explained (jive) for integrated analysis of multiple data types. *Annals of Application Statistics* 7(1), 523–542.
- Mshaik, R., Simonet, J., Georgievski, A., et al., 2021. Hsp90 inhibitor nvp-bep800 affects stability of src kinases and growth of t-cell and b-cell acute lymphoblastic leukemias. *Blood Cancer Journal* 11(61). URL: <https://www.nature.com/articles/s41408-021-00450-2>, doi:10.1038/s41408-021-00450-2.
- Norris, J.L., Farrow, M.A., Gutierrez, D.B., et al., 2017. Integrated, high-throughput, multiomics platform enables data-driven construction of cellular responses and reveals global drug mechanisms of action. *Journal of Proteome Research* 16(3), 1364–1375. doi:<https://doi.org/10.1021/acs.jproteome.6b01004>.
- Passemier, D., Yao, J.F., 2014. Estimation of the number of spikes, possibly equal, in the high-dimensional case. *Journal of Multivariate Analysis* 127, 173–183.
- Reuter, J.A., Spacek, D., Snyder, M.P., 2015. High-throughput sequencing technologies. *Molecular Cell* 58(4), 586–597. doi:10.1016/j.molcel.2015.05.004.
- Smilde, A.K., Westerhuis, J.A., de Jong, S., 2003. A framework for sequential multiblock component methods. *Journal of Chemometrics* 17, 323–337.
- Subramanian, I., Verma, S., Kumar, S., Jere, A., Anamika, K., 2020. Multi-omics data integration, interpretation, and its application. *Bioinformatics and Biology Insights* URL: <https://journals.sagepub.com/doi/full/10.1177/1177932219899051>, doi:10.1177/1177932219899051.
- VanDeun, K., Smilde, A.K., van der Werf, M.J., Kiers, H.A., VanMechelen, I., 2009. A structured overview of simultaneous component based data integration. *BMC Bioinformatics* 10, 246.
- Wang, C., Youle, R.J., 2014. The role of mitochondria in apoptosis. *Annu Rev Genet.* 43, 95–118.

Ye, K., Lim, L.H., 2016. Schubert varieties and distances between subspaces of different dimensions. *SIAM Journal of Matrix Analysis and Applications* 37(3), 1176–1197.

Zhang, Y., Hunter, T., 2014. Roles of chk1 in cell biology and cancer therapy. *International Journal of Cancer* 134(5), 1013–1023.

SUPPLEMENTARY MATERIAL

A. Proofs

A.1. Some basic facts for proof

As it is the most elementary fact, we begin by recapitulating Lemma 2 and show its proof.

Lemma 2. *For $i, j \in \mathcal{I}_K$ and $S_i \cap S_j \neq \phi$, $[W_i] \perp [W_j]$.*

Proof. From the definition of the partially-joint score subspace, $[W_i]$, we immediately find that

$$[W_i] \perp [W_j], \quad i, j \in \mathcal{I}_K \text{ and } S_j \cap S_i \neq \phi$$

by the range-kernel complementarity property of the vector space projection transformation. \square

We denote $\mathcal{I}_{<i} = \{j : j < i, S_j \cap S_i \neq \phi\}$. Hereafter $\mathcal{N}(T)$ is the null space of a linear transformation T of \mathbb{R}^n and $\mathcal{R}(T)$ its range space.

Lemma A.1. *For $i \in \mathcal{I}_K$, we have $\mathcal{N}(\bigcirc_{k \in \mathcal{I}_{<i}} P_k^\perp) = \bigoplus_{k \in \mathcal{I}_{<i}} [W_k]$.*

Proof. Let $v \in \bigoplus_{k \in \mathcal{I}_{<i}} [W_k]$. Then there exists a unique $\{v_k\}_{k \in \mathcal{I}_{<i}}$ with $v_k \in [W_k]$ such that the sum of all v_k is v . For each $j_1 \in \mathcal{I}_{<i}$ and $v_{j_1} \in [W_{j_1}]$, it can be easily checked that $(\bigcirc_{k \in \mathcal{I}_{<j_1}} P_k^\perp)(v_{j_1}) = \{0\}$ and then $(\bigcirc_{k \in \mathcal{I}_{<i}} P_k^\perp)(v_{j_1}) = \{0\}$ follows. Thus $(\bigcirc_{k \in \mathcal{I}_{<i}} P_k^\perp)(v) = \{0\}$ and $\mathcal{N}(\bigcirc_{k \in \mathcal{I}_{<i}} P_k^\perp) \supset \bigoplus_{k \in \mathcal{I}_{<i}} [W_k]$.

Conversely, let $v' \notin \bigoplus_{k \in \mathcal{I}_{<i}} [W_k]$. Then there exists a unique $\{v_k\}_{k \in \mathcal{I}_{<i}}$ with $v_k \in [W_k]$ and non-zero $a \in (\bigoplus_{k \in \mathcal{I}_{<i}} [W_k])^\perp$ such that v' is the sum of all v_k and a . For each $j_1 \in \mathcal{I}_{<i}$ and $v_{j_1} \in [W_{j_1}]$, we have $(\bigcirc_{k \in \mathcal{I}_{<i}} P_k^\perp)(v_{j_1}) = \{0\}$ as before. Since $a \perp [W_{k''}]$ for any $k'' \in \mathcal{I}_{<i}$, we also have $(\bigcirc_{k \in \mathcal{I}_{<i}} P_k^\perp)(a) \neq 0$. Thus we have $(\bigcirc_{k \in \mathcal{I}_{<i}} P_k^\perp)(v') \neq \{0\}$ and $\mathcal{N}(\bigcirc_{k \in \mathcal{I}_{<i}} P_k^\perp) \subset \bigoplus_{k \in \mathcal{I}_{<i}} [W_k]$. \square

Lemma A.2. *For $i \in \mathcal{I}_K$, we have $\bigoplus_{k \in \mathcal{I}_{<i}} [W_k] = \bigoplus_{k \in \mathcal{I}_{<i}} (\bigcap_{k' \in S_k} [V_{k'}])$.*

Proof. We give a proof by induction on k . If $k = 1$, there is nothing to prove. If $k = 2$, $[W_1] = \bigcap_{k' \in S_1} [V_{k'}]$, so the statement is true for $k = 1, 2$.

For any $k \geq 3$, suppose the statement holds, that is,

$$\bigoplus_{j \in \mathcal{I}_{<m}} [W_j] = \bigoplus_{j \in \mathcal{I}_{<m}} (\bigcap_{k' \in S_j} [V_{k'}])$$

for all $1 \leq m \leq k$. Let \tilde{k} be the largest element in $\mathcal{I}_{<k+1}$. We denote $P = \bigcirc_{k' \in \mathcal{I}_{<\tilde{k}}} P_{k'}^\perp$ and P^\perp , the projection onto $\mathcal{N}(P)$ of \mathbb{R}^n . Then, we have

$$\begin{aligned} +_{j \in \mathcal{I}_{<k+1}} (\cap_{k' \in S_j} [V_{k'}]) &= \oplus_{j \in \mathcal{I}_{<\tilde{k}}} [W_j] + \cap_{k' \in S_{\tilde{k}}} [V_{k'}] \\ &= \oplus_{j \in \mathcal{I}_{<\tilde{k}}} [W_j] + P(\cap_{k' \in S_{\tilde{k}}} [V_{k'}]) + P^\perp(\cap_{k' \in S_{\tilde{k}}} [V_{k'}]) \end{aligned}$$

Indeed, $P^\perp(\cap_{k' \in S_{\tilde{k}}} [V_{k'}]) \subset \mathcal{N}(P)$ and $\mathcal{N}(P) = \oplus_{k' \in \mathcal{I}_{<\tilde{k}}} [W_{k'}]$ by the previous lemma. Thus

$$\begin{aligned} +_{j \in \mathcal{I}_{<k+1}} (\cap_{k' \in S_j} [V_{k'}]) &= \oplus_{j \in \mathcal{I}_{<\tilde{k}}} [W_j] + P(\cap_{k' \in S_{\tilde{k}}} [V_{k'}]) \\ &= \oplus_{j \in \mathcal{I}_{<\tilde{k}}} [W_j] \oplus [W_{\tilde{k}}] \\ &= \oplus_{j \in \mathcal{I}_{<k+1}} [W_j]. \end{aligned}$$

Therefore the statement holds for any $k \geq 3$ and the proof is completed. \square

Lemma A.3. For $k = 1, \dots, K$, $+_{i \in \{k \in S_i\}} [W_{S_i}] = [V_k]$.

Proof. In Lemma A.2, we set i such that $S_i = \{k\}$. Then $\mathcal{I}_{<i} = \{j : k \in S_j, |S_j| > 1\}$ and $\oplus_{j \in \mathcal{I}_{<i}} [W_j] = +_{j \in \mathcal{I}_{<i}} (\cap_{k' \in S_j} [V_{k'}])$. The proof goes similarly as in Lemma A.2. Let \tilde{i} be the largest element in $\mathcal{I}_{<i}$. We denote $P = \bigcirc_{k' \in \mathcal{I}_{<\tilde{i}}} P_{k'}^\perp$ and P^\perp , the projection onto $\mathcal{N}(P)$ of \mathbb{R}^n .

$$\begin{aligned} +_{j \in \mathcal{I}_{<i} \cup S_i} (\cap_{k' \in S_j} [V_{k'}]) &= \oplus_{j \in \mathcal{I}_{<i}} [W_j] + \cap_{k' \in S_i} [V_{k'}] \\ &= \oplus_{j \in \mathcal{I}_{<i}} [W_j] + P(\cap_{k' \in S_i} [V_{k'}]) + P^\perp(\cap_{k' \in S_i} [V_{k'}]) \\ &= \oplus_{j \in \mathcal{I}_{<i}} [W_j] + P(\cap_{k' \in S_i} [V_{k'}]) \\ &= \oplus_{j \in \mathcal{I}_{<i}} [W_j] \oplus [W_i] \\ &= \oplus_{j \in \mathcal{I}_{<i} \cup S_i} [W_j]. \end{aligned}$$

By the set inclusion-exclusion principle, as $\mathcal{I}_{<i} \cup S_i$ involves every index-set that contains k , it is immediate that $+_{j \in \mathcal{I}_{<i} \cup S_i} (\cap_{k' \in S_j} [V_{k'}]) = [V_k]$. \square

A.2. Proof of Theorem 1

Proof. We claim that $\text{rank}([W_i])$ is uniquely determined. By Sylvester's law of nullity, we have

$$\text{rank}([W_i]) = \text{rank}(\cap_{k \in S_i} [V_k]) - \text{rank}(\mathcal{N}(\bigcirc_{j \in \mathcal{I}_{<i}} P_j^\perp) \cap (\cap_{k \in S_i} [V_k])),$$

where $\mathcal{I}_{<i} = \{j : j < i, S_j \cap S_i \neq \emptyset\}$ as before. By lemma A.1 and A.2, Sylvester's law of nullity for our theorem is restated as

$$\text{rank}([W_i]) = \text{rank}(\cap_{k \in S_i} [V_k]) - \text{rank}((+_{k \in \mathcal{I}_{<i}} (\cap_{k' \in S_k} [V_{k'}])) \cap (\cap_{k \in S_i} [V_k])).$$

We want to make this expression in a more explicit form. For that, we suggest the following assertions.

Let $l = |S_i|$. We set $[I_l] = +_{k \in \{k : |S_k| > l\}} (\cap_{k' \in S_k} [V_{k'}])$. The projection onto $[I_l]$ in \mathbb{R}^n is denoted by P_{I_l} and the projection onto $[I_l]^\perp$ is denoted by $P_{I_l}^\perp$. Moreover, we consider an index set $\mathcal{J}_{i,>l} = \mathcal{I}_{<i} \cap \{k : |S_k| > l\}$ and let $[J_i] = +_{k \in \mathcal{J}_{i,>l}} (\cap_{k' \in S_k} [V_{k'}])$. The projection onto $[J_i]$ in \mathbb{R}^n is denoted by P_{J_i} and the projection onto $[J_i]^\perp$ by $P_{J_i}^\perp$. Finally, we define $\mathcal{J}_{i,l} = \mathcal{I}_{<i} \cap \{k : |S_k| = l\}$.

Lemma A.4. $P_{I_l}^\perp = P_{I_l}^\perp \circ P_{J_i}^\perp$.

Proof. Trivial from the fact $\mathcal{N}(P_{J_i}^\perp) \subset \mathcal{N}(P_{I_l}^\perp)$. \square

Lemma A.5. *If $v_j \in P_{J_i}^\perp(\cap_{k' \in S_j} [V_{k'}])$ with $j \in \mathcal{J}_{i,l} \setminus \mathcal{J}'_{i,l}$, then $v_j \in (\cap_{k' \in S_j} [V_{k'}]) \cap (\cap_{k' \in S_m} [V_{k'}])$ for some $m < i$, $m \neq j$ such that $S_m \cap S_i = \{0\}$ and not for any $m < i$, $m \neq j$ such that $S_m \cap S_i \neq \{0\}$.*

Proof. Consider the cases

- (1) $v_j \in (\cap_{k' \in S_j} [V_{k'}]) \cap (\cap_{k' \in S_m} [V_{k'}])$ for some $m < i$, $m \neq j$ such that $S_m \cap S_i \neq \{0\}$ but not for any $S_m \cap S_i = \{0\}$,
- (2) $(\cap_{k' \in S_j} [V_{k'}]) \cap (\cap_{k' \in S_m} [V_{k'}]) = \{0\}$ for only $m \in \mathcal{J}_{i,l}$

In case (1), v_j becomes automatically an element of $\cap_{k' \in S_t} [V_{k'}]$ such that $S_j \subset S_t$ and $S_m \subset S_t$. Then $v_j \in [I_i]$ since $S_i \cap S_t \neq \emptyset$ and $|S_t| > |S_i|$, and this is a contradiction. In case (2), $v_j \notin \mathcal{R}(P_{I_l})$ and this is contradict to the assumption. \square

Proposition A.1. *If $[V_k]_{k \in \mathcal{K}}$ is relatively independent, then $+_{k \in \mathcal{J}_{i,l}} P_{J_i}^\perp(\cap_{k' \in S_k} [V_{k'}])$ and $P_{J_i}^\perp(\cap_{k \in S_i} [V_k])$ are independent.*

Proof. We want to show that the relative independence of $[V_k]_{k \in \mathcal{K}}$ is violated if $+_{k \in \mathcal{J}_{i,l}} P_{J_i}^\perp(\cap_{k' \in S_k} [V_{k'}])$ and $P_{J_i}^\perp(\cap_{k \in S_i} [V_k])$ are linearly dependent. Suppose that there is nonzero $v \in +_{k \in \mathcal{J}_{i,l}} P_{J_i}^\perp(\cap_{k' \in S_k} [V_{k'}]) \cap P_{J_i}^\perp(\cap_{k \in S_i} [V_k])$ with $l = |S_i|$. We are going to show that $+_{k \in \mathcal{J}_{i,l}} P_{J_i}^\perp(\cap_{k' \in S_k} [V_{k'}]) \cap P_{J_i}^\perp(\cap_{k \in S_i} [V_k])$ is not $\{0\}$ in the following cases.

First we exclude the case where $P_{I_l}^\perp(\cap_{k' \in S_i} [V_{k'}]) = \{0\}$. If so we have $\cap_{k' \in S_i} [V_{k'}] = \oplus_{k'' \in \{k'' : S_i \subset S_{k''}\}} [W_{k''}] = +_{k'' \in \{k'' : S_i \subset S_{k''}\}} [V_{k''}]$, then $\cap_{k' \in S_i} [V_{k'}]$ itself is in $[I_i] = \mathcal{N}(P_{J_i}^\perp)$.

Next, under the assumption that $P_{I_l}^\perp(\cap_{k' \in S_i} [V_{k'}]) \neq \{0\}$, we run through the following situations. Now on $\mathcal{J}'_{i,l} = \{k : |S_k| = l, k \in \mathcal{I}_{<i}, P_{I_i}^\perp(S_k) \neq \{0\}\}$.

(i) $|\mathcal{J}_{i,l}| = 0$: There is nothing to prove.

(ii) $|\mathcal{J}_{i,l}| = 1$ and $|\mathcal{J}'_{i,l}| = 0$:

We will show that this case is vacuous. Suppose there exist nonzero $v \in P_{J_i}^\perp(\cap_{k' \in S_i} [V_{k'}]) \cap P_{J_i}^\perp(\cap_{k' \in S_k} [V_{k'}])$ with $k \in \mathcal{J}_{i,l}$. As $P_{I_l}^\perp(\cap_{k' \in S_k} [V_{k'}]) = \{0\}$, we can deduce that $P_{I_l}^\perp(v) = 0$.

We pick a vector u in $\cap_{k' \in S_j} [V_{k'}]$ such that $S_i \subset S_j$ and $S_j \subset S_k$. As $\cap_{k' \in S_j} [V_{k'}] \subset \cap_{k' \in S_i} [V_{k'}]$ and $\cap_{k' \in S_j} [V_{k'}] \subset \cap_{k' \in S_k} [V_{k'}]$, we have $u \in (\cap_{k' \in S_i} [V_{k'}]) \cap (\cap_{k' \in S_k} [V_{k'}])$. As $S_i \cap S_j \neq \emptyset$, we observe that $\cap_{k' \in S_i} [V_{k'}] \subset [I_i] = \mathcal{N}(P_{J_i}^\perp)$.

$$\begin{aligned} u &\in P_{J_i}((\cap_{k' \in S_i} [V_{k'}]) \cap (\cap_{k' \in S_k} [V_{k'}])) \\ &\subset P_{J_i}(\cap_{k' \in S_i} [V_{k'}]) \cap P_{J_i}(\cap_{k' \in S_k} [V_{k'}]). \end{aligned}$$

Let $w = u + v$. Since $u \in P_{J_i}(\cap_{k' \in S_k} [V_{k'}])$ and $v \in P_{J_i}^\perp(\cap_{k' \in S_k} [V_{k'}])$ with respect to S_k and the same for S_i , we find that $w \in (\cap_{k' \in S_i} [V_{k'}]) \cap (\cap_{k' \in S_k} [V_{k'}])$, and then, $w \in [I_i] = \mathcal{N}(P_{J_i}^\perp)$. But this forces $P_{J_i}^\perp(w) = v$ and v to be zero and leads to vacuity.

(iii) $|\mathcal{J}_{i,l}| = 1$ and $|\mathcal{J}'_{i,l}| = 1$:

Suppose there is nonzero $v \in P_{J_i}^\perp(\cap_{k' \in S_k} [V_{k'}])$ with $k \in \mathcal{J}_{i,l}$. From Lemma A.4, we have $P_{I_l}^\perp(v) \in P_{I_l}^\perp(\cap_{k' \in S_k} [V_{k'}])$. By the same argument, $P_{I_l}^\perp(v) \in P_{I_l}^\perp(\cap_{k' \in S_i} [V_{k'}])$. Then there is a nonzero $P_{I_l}^\perp(v) \in P_{I_l}^\perp(\cap_{k' \in S_i} [V_{k'}]) \cap P_{I_l}^\perp(\cap_{k' \in S_k} [V_{k'}])$.

(iv) $|\mathcal{J}_{i,l}| \geq 2$, $|\mathcal{J}'_{i,l}| = 0$ and $v \in P_{J_i}^\perp(\cap_{k' \in S_k} [V_{k'}])$ with some $k \in \mathcal{J}_{i,l}$: the same as case (ii).

(v) $|\mathcal{J}_{i,l}| \geq 2$, $|\mathcal{J}'_{i,l}| = 0$ and $v \notin P_{J_i}^\perp(\cap_{k' \in S_k} [V_{k'}])$ with any of $k \notin \mathcal{J}_{i,l}$:

We will show that this case is a generalization of case (ii) and also vacuous. As $v \in +_{k \in \mathcal{J}_{i,l}} P_{J_i}^\perp(\cap_{k' \in S_k} [V_{k'}])$, we express

$$v = \sum_{j \in \mathcal{J}_{i,l}} a_j v_j$$

for each $a_j \in \mathbb{R}$ (at least two of them are nonzero) and $v_j \in P_{J_i}^\perp(\cap_{k' \in S_j} [V_{k'}])$.

By Lemma A.5, for each v_j for $j \in \mathcal{J}_{i,l}$, we can find $S_{m,j}$ such that $v_j \in S_{m,j}$ and $m < i$, $m \neq j$, $S_m \cap S_i = \{0\}$. And this also implies that there exists certain $S_{t,j}$ and $v_j \in S_{t,j}$ such that $S_j \subset S_{t,j}$ and $S_{m,j} \subset S_{t,j}$. Here we point out that as $S_{t,j} \cap S_i \neq \phi$, since $S_j \cap S_i \neq \phi$. Then all $\cap_{k' \in S_{t,j}} [V_{k'}]$ for $j \in \mathcal{J}_{i,l}$ and their linear combinations are subsets of $[I_i]$. This leads to the conclusion $v \in [I_i]$ and shows the vacuity of this case.

(vi) $|\mathcal{J}_{i,l}| \geq 2$, $|\mathcal{J}'_{i,l}| \geq 1$ and $v \in P_{J_i}^\perp(\cap_{k' \in S_k} [V_{k'}])$ with some $k \in \mathcal{J}_{i,l}$:
If $k \in \mathcal{J}'_{i,l}$, then the same as the case (iii). If $k \notin \mathcal{J}'_{i,l}$, then the same as the case (ii).

(vii) $|\mathcal{J}_{i,l}| \geq 2$, $|\mathcal{J}'_{i,l}| \geq 1$ and $v \notin P_{J_i}^\perp(\cap_{k' \in S_k} [V_{k'}])$ with any of $k \in \mathcal{J}_{i,l}$:
As $v \in +_{k \in \mathcal{J}_{i,l}} P_{J_i}^\perp(\cap_{k' \in S_k} [V_{k'}])$, we express

$$v = \sum_{j \in \mathcal{J}_{i,l}} a_j v_j$$

for each $a_j \in \mathbb{R}$ (at least two of them are nonzero) and $v_j \in P_{J_i}^\perp(\cap_{k' \in S_j} [V_{k'}])$. Note that if $a_{j'} = 0$ for all $j' \in \mathcal{J}'_{i,l}$, then this case is essentially the same as case (v), so we only consider the situation at least one $a_{j'} \neq 0$ for $j' \in \mathcal{J}'_{i,l}$.

By Lemma A.5 and its consequences in case (v), for each $j \in \mathcal{J}_{i,l} \setminus \mathcal{J}'_{i,l}$, there exists $S_{t,j}$ and $v_j \in S_{t,j}$ such that $S_j \subset S_{t,j}$ and $S_{m,j} \subset S_{t,j}$. As previously discussed, $\cap_{k' \in S_{t,j}} [V_{k'}]$ for $j \in \mathcal{J}_{i,l} \setminus \mathcal{J}'_{i,l}$ is a subset of $[I_i]$. So we rule out the terms involving $j \in \mathcal{J}_{i,l} \setminus \mathcal{J}'_{i,l}$ and then

$$P_{I_i}^\perp(v) = \sum_{j' \in \mathcal{J}'_{i,l}} a_{j'} P_{I_i}^\perp(v_{j'}).$$

Since each $\cap_{k' \in S_{j'}} [V_{k'}] \neq \{0\}$ for $j \in \mathcal{J}'_{i,l}$ is a subset of $[I_i]$ and at least one $a_{j'} \neq 0$, we deduce that $P_{I_i}^\perp(v)$ is non-zero. Therefore, the relative independence is violated.

□

Now the last term in the RHS of our law of nullity is re-expressed as

$$\begin{aligned}
& (+_{k \in \mathcal{I}_{< i}} (\cap_{k' \in S_k} [V_{k'}])) \cap (\cap_{k \in S_i} [V_k]) \tag{A.1} \\
& = ((+_{k \in \mathcal{J}_{i, < l}} (\cap_{k' \in S_k} [V_{k'}])) \oplus (+_{k \in \mathcal{J}_{i, l}} P_{J_i}^\perp (\cap_{k' \in S_k} [V_{k'}]))) \cap (\cap_{k \in S_i} [V_k]) \\
& = ((+_{k \in \mathcal{J}_{i, < l}} (\cap_{k' \in S_k} [V_{k'}])) \oplus (+_{k \in \mathcal{J}_{i, l}} P_{J_i}^\perp (\cap_{k' \in S_k} [V_{k'}]))) \\
& \quad \cap (P_{J_i} (\cap_{k \in S_i} [V_k]) \oplus P_{J_i}^\perp (\cap_{k \in S_i} [V_k]))
\end{aligned}$$

In Proposition A.1, we have observed that $+_{k \in \mathcal{J}_{i, l}} P_{J_i}^\perp (\cap_{k' \in S_k} [V_{k'}])$ and $P_{J_i}^\perp (\cap_{k \in S_i} [V_k])$ are independent. As $P_{J_i} (\cap_{k \in S_i} [V_k]) \subset +_{k \in \mathcal{J}_{i, < l}} (\cap_{k' \in S_k} [V_{k'}])$, the term (A.1) becomes

$$(+_{k \in \mathcal{I}_{< i}} (\cap_{k' \in S_k} [V_{k'}])) \cap (\cap_{k \in S_i} [V_k]) = (+_{k \in \mathcal{J}_{i, < l}} (\cap_{k' \in S_k} [V_{k'}])) \cap (P_{J_i} (\cap_{k \in S_i} [V_k])).$$

Finally, we have demonstrated

$$\begin{aligned}
\text{rank}([W_i]) &= \text{rank}(\cap_{k \in S_i} [V_k]) - \text{rank} \left((+_{k \in \mathcal{I}'_{< i}} (\cap_{k' \in S_k} [V_{k'}])) \cap (\cap_{k \in S_i} [V_k]) \right) \\
&= \text{rank}(\cap_{k \in S_i} [V_k]) \\
&\quad - \text{rank} \left((+_{k \in \mathcal{J}_{i, < l}} (\cap_{k' \in S_k} [V_{k'}])) \cap (P_{J_i} (\cap_{k \in S_i} [V_k])) \cap (\cap_{k \in S_i} [V_k]) \right) \\
&= \text{rank}(\cap_{k \in S_i} [V_k]) - \text{rank} (P_{J_i} (\cap_{k \in S_i} [V_k])).
\end{aligned}$$

It is notable that the determination of $\text{rank}([W_i])$ depends only on $\mathcal{J}_{i, > l}$, that is, the set of indices j such that $|S_j| > |S_i|$ and $S_j \cap S_i \neq \phi$. In other words, it does not depend on any index-sets of the same size as S_i and their orderings.

As partially-joint score subspaces $[W_i]$ are constructed recursively and the determination of each $[W_i]$'s rank only depends on $\mathcal{J}_{i, > l}$, not on the ordering index-sets of size $l = |S_i|$, we conclude that the set of pairs $\{(S_i, r(S_i)) : i \in \mathcal{I}_K\}$ is unique. \square

A.3. Proof of Theorem 2

Proof. We give a proof recursively on $l \in \mathcal{K}$. If $l = K$, there only exists $[W_1] = \cap_{k' \in S_1} [V_{k'}]$ for $S_1 = \mathcal{K}$, so there is nothing to prove. If $l = K - 1$, by absolute orthogonality, all $P_1^\perp (\cap_{k' \in S_i} [V_{k'}])$ are orthogonal each other for $i = \{2, \dots, K + 1\}$. Therefore, in determining each $[W_i]$ for $i = \{2, \dots, K + 1\}$, other $[W_t]$ for $t \in \mathcal{J}_{i, 2} = \mathcal{I}_{< i} \cap \{i' : |S_{i'}| = 2\}$ does not affect on the construction of $[W_i]$.

For any $l \leq K - 2$, suppose the statement holds, that is, a partially-joint score subspace $[W_j]$ such that $|S_j| = l' > l$ is uniquely determined only by

$[W_{j'}]$ for $S_{j'} > S_j$. For each index $i \in \mathcal{J}_l = \{i' : |S_{i'}| = l\}$ (regardless of ordering), we have $P_{I_i}(\cap_{k' \in S_i} [V_{k'}]) = P_{J_i}(\cap_{k' \in S_i} [V_{k'}])$ by absolute orthogonality. Then among all indices $i' \in \mathcal{J}_l$, $P_{J_{i'}}^\perp(\cap_{k' \in S_{i'}} [V_{k'}])$ are orthogonal each other.

Suppose an ordering on the set of all index-sets of size l is given, denoted by $(S_{i_1}, \dots, S_{i_h})$ with $h = {}_K C_l$. For i_1 , $[W_{i_1}]$ is just determined as $P_{J_{i_1}}^\perp(\cap_{k' \in S_{i_1}} [V_{k'}])$. Next for i_2 , as $[W_{i_1}]$ and $P_{J_{i_2}}^\perp(\cap_{k' \in S_{i_2}} [V_{k'}])$ are orthogonal, we check that $P_{i_1}^\perp \circ P_{J_{i_2}}^\perp(\cap_{k' \in S_{i_2}} [V_{k'}]) = P_{J_{i_2}}^\perp(\cap_{k' \in S_{i_2}} [V_{k'}])$. Thus $[W_{i_2}]$ is determined regardless of $[W_{i_1}]$. In recursive manner, for $i \in \{i_3, \dots, i_h\}$, $[W_i]$ is determined regardless of all $[W_{i'}]$ for $i' \in \mathcal{J}_{i,l}$, or in other word, is uniquely determined as $P_{J_i}^\perp(\cap_{k' \in S_i} [V_{k'}])$ depending only on $[W_{j'}]$ s for $S_{j'} > l$. \square

A.4. Proof of Corollary 1

Proof. From the discussions of Section 2, we know that $[W_{(k)}]$ is indeed the score subspace of Z_k for each $k = 1, \dots, K$. Thus, given unique $[W_i]$'s for $i \in \mathcal{I}_{(k)}$ from Theorem 2, the subspace $[U_{(k),i}]$ generated by $U_{(k),i}$ is unique. \square

A.5. Examples

The following two examples presents the cases where relative independence is satisfied and not:

Example A.1. Let $K = 3$, $n = 4$ and

$$V_1 = \begin{pmatrix} 1 & 0 \\ 0 & 1 \\ 0 & 0 \\ 0 & 0 \end{pmatrix}, \quad V_2 = \begin{pmatrix} 1 & 0 \\ 0 & 1/\sqrt{2} \\ 0 & 1/\sqrt{2} \\ 0 & 0 \end{pmatrix}, \quad V_3 = \begin{pmatrix} 1 & 0 \\ 0 & 0 \\ 0 & 1/\sqrt{2} \\ 0 & 1/\sqrt{2} \end{pmatrix}$$

then $[I_1] = [(1, 0, 0, 0)^T]$ and $P_{I_1}^\perp[V_1] = [(0, 1, 0, 0)^T]$, $P_{I_1}^\perp[V_2] = [(0, 1/\sqrt{2}, 1/\sqrt{2}, 0)^T]$ and $P_{I_1}^\perp[V_3] = [(0, 0, 1/\sqrt{2}, 1/\sqrt{2})^T]$ are linearly independent. Thus $\{[V_1], [V_2], [V_3]\}$ is relatively independent.

Example A.2. Let $K = 3$, $n = 4$ and

$$V_1 = \begin{pmatrix} 1 & 0 \\ 0 & 1 \\ 0 & 0 \\ 0 & 0 \end{pmatrix}, \quad V_2 = \begin{pmatrix} 1 & 0 \\ 0 & 1/\sqrt{2} \\ 0 & 1/\sqrt{2} \\ 0 & 0 \end{pmatrix}, \quad V_3 = \begin{pmatrix} 1 & 0 & 0 \\ 0 & 0 & 0 \\ 0 & 1 & 1/\sqrt{2} \\ 0 & 0 & 1/\sqrt{2} \end{pmatrix}$$

As $P_{I_1}^\perp[V_3] \cap (P_{I_1}^\perp[V_1] + P_{I_1}^\perp[V_2]) = [(0, 0, 1, 0)^T]$ is not empty, thus $\{[V_1], [V_2], [V_3]\}$ is not relatively independent.

We present the following examples that support Theorem 1, that relative independence indeed guarantee the uniqueness of the brief version of *partially-joint structure* $\mathfrak{S}_0 = \{(S_i, r(S_i)) : i \in \mathcal{I}_K, r(S_i) > 0\}$.

Example A.3 (cont'd from Example A.1.). *Under the ordering $S_1 = \{1, 2, 3\}, S_5 = \{1\}, S_6 = \{2\}, S_7 = \{3\}$, we obtain $[W_1] = [(1, 0, 0, 0)^T]$, $[W_5] = [(0, 1, 0, 0)^T]$, $[W_6] = [(0, 0, 1, 0)^T]$ and $[W_7] = [(0, 0, 0, 1)^T]$. Then we have*

$$\mathfrak{S}_0 = \{(\{1, 2, 3\}, 1), (\{1\}, 1), (\{2\}, 1), (\{3\}, 1)\}.$$

On the other hand, in the case $S_1 = \{1, 2, 3\}, S_5 = \{2\}, S_6 = \{1\}, S_7 = \{3\}$, we obtain $[W_1] = [(1, 0, 0, 0)^T]$, $[W_5] = [(0, 1/\sqrt{2}, 1/\sqrt{2}, 0)^T]$, $[W_6] = [(0, -1/\sqrt{2}, 1/\sqrt{2}, 0)^T]$ and $[W_7] = [(0, 0, 0, 1)^T]$. The partially-joint structure is still the same as above.

Example A.4 (cont'd from Example A.2.). *Under the ordering $S_1 = \{1, 2, 3\}, S_5 = \{1\}, S_6 = \{2\}, S_7 = \{3\}$, we obtain $[W_1] = [(1, 0, 0, 0)^T]$, $[W_5] = [(0, 1, 0, 0)^T]$, $[W_6] = [(0, 0, 1, 0)^T]$ and $[W_7] = [(0, 0, 0, 1)^T]$. The partially-joint structure is*

$$\mathfrak{S}_0 = \{(\{1, 2, 3\}, 1), (\{1\}, 1), (\{2\}, 1), (\{3\}, 1)\}.$$

On the other hand, in the case $S_1 = \{1, 2, 3\}, S_5 = \{3\}, S_6 = \{2\}, S_7 = \{1\}$, we obtain $[W_1] = [(1, 0, 0, 0)^T]$, $[W_5] = [(0, 1, 0, 0)^T, (0, 0, 1/\sqrt{2}, 1/\sqrt{2})^T]$, $[W_6] = [(0, 0, 1/\sqrt{2}, -1/\sqrt{2})^T]$ and $[W_7] = \{0\}$. This time, the partially-joint structure is

$$\mathfrak{S}_0 = \{(\{1, 2, 3\}, 1), (\{1\}, 0), (\{2\}, 1), (\{3\}, 2)\}.$$

We also present the following examples that support Theorem 2, that absolute orthogonality guarantee the uniqueness of the partially-joint score subspaces.

Example A.5. *Let $K = 4, n = 7$ and*

$$\begin{aligned} V_1 &= (0 \ 0 \ 1 \ 0 \ 0 \ 0)^T \\ V_2 &= (0 \ 0 \ 0 \ 1 \ 0 \ 0)^T \\ V_3 &= \begin{pmatrix} 1/\sqrt{2} & 1/\sqrt{2} & 0 & 0 & 0 & 0 \\ 0 & 0 & 0 & 0 & 1 & 0 \end{pmatrix}^T \\ V_4 &= \begin{pmatrix} 1/\sqrt{2} & 1/\sqrt{2} & 0 & 0 & 0 & 0 \\ 0 & 0 & 0 & 0 & 0 & 1 \end{pmatrix}^T. \end{aligned}$$

This example satisfies absolute orthogonality. Between under two orderings ($S_{11} = \{3, 4\}, S_{12} = \{1\}, S_{13} = \{2\}$) and ($S_{11} = \{3, 4\}, S_{12} = \{2\}, S_{13} = \{1\}$), the determinations of $[W_{12}]$ and $[W_{13}]$ are the same.

Example A.6. Let $K = 4, n = 7$ and

$$\begin{aligned} V_1 &= (1/2\sqrt{2} \quad \sqrt{3}/2\sqrt{2} \quad 1/\sqrt{2} \quad 0 \quad 0 \quad 0)^T \\ V_2 &= (\sqrt{3}/2\sqrt{2} \quad 1/2\sqrt{2} \quad 0 \quad 1/\sqrt{2} \quad 0 \quad 0)^T \\ V_3 &= \begin{pmatrix} 1/\sqrt{2} & 1/\sqrt{2} & 0 & 0 & 0 & 0 \\ 0 & 0 & 0 & 0 & 1 & 0 \end{pmatrix}^T \\ V_4 &= \begin{pmatrix} 1/\sqrt{2} & 1/\sqrt{2} & 0 & 0 & 0 & 0 \\ 0 & 0 & 0 & 0 & 0 & 1 \end{pmatrix}^T. \end{aligned}$$

This example satisfies relative orthogonality, but not absolute orthogonality. Between under two orderings ($S_{11} = \{3, 4\}, S_{12} = \{1\}, S_{13} = \{2\}$) and ($S_{11} = \{3, 4\}, S_{12} = \{2\}, S_{13} = \{1\}$), the determinations of $[W_{12}]$ and $[W_{13}]$ are not the same because $[V_1]$ and $[V_2]$ are not orthogonal and $[W_{11}] = (1/\sqrt{2}, 1/\sqrt{2}, 0, 0, 0, 0)^T$ does not have an effect on the determination of $[W_{12}]$ and $[W_{13}]$ by definition.

B. Additional Information on Simulation Study

B.1. Example of the Measure of Dissimilarity between Two Partially-Joint Structures

For the comparison between two partially-joint structure, we devised a following concept of the measure of dissimilarity between partially-joint structures.

First, we introduce a *partially-joint structure matrix* \hat{T} for a (brief version of) partially-joint structure $\hat{\mathfrak{S}}_0$, a matrix each of whose columns indicates an identified index-set among datasets and each of whose elements show whether the corresponding dataset belongs to that index-set. For example, when $K = 3$, if the estimated partially-joint structure is

$$\hat{\mathfrak{S}}_0 = \{(\{1, 2, 3\}, 2), (\{1, 2\}, 1), (\{1, 3\}, 1), (\{2, 3\}, 1), (\{3\}, 1)\},$$

then

$$\hat{T} = \begin{pmatrix} 1 & 1 & 1 & 1 & 0 & 0 \\ 1 & 1 & 1 & 0 & 1 & 0 \\ 1 & 1 & 0 & 1 & 1 & 1 \end{pmatrix}.$$

Next, consider two partially-joint structure matrices $\widehat{T}_1 \in \{0, 1\}^{n \times m_1}$ and $\widehat{T}_2 \in \{0, 1\}^{n \times m_2}$. Discarding all the identical columns between \widehat{T}_1 and \widehat{T}_2 , we denote the remaining columns \widetilde{T}_1 and \widetilde{T}_2 . For example, from

$$\widehat{T}_1 = \begin{bmatrix} 1 & 1 \\ 1 & 1 \\ 1 & 0 \end{bmatrix}, \quad \widehat{T}_2 = \begin{bmatrix} 1 & 1 & 0 \\ 1 & 1 & 1 \\ 1 & 1 & 1 \end{bmatrix},$$

we obtain

$$\widetilde{T}_1 = \begin{bmatrix} 1 \\ 1 \\ 0 \end{bmatrix}, \quad \widetilde{T}_2 = \begin{bmatrix} 1 & 0 \\ 1 & 1 \\ 1 & 1 \end{bmatrix}.$$

For each remaining column of \widehat{T}_1 (or \widehat{T}_2), find the closest column of \widehat{T}_2 (or \widehat{T}_1) in the Frobenius norm sense. The measure of dissimilarity between \widehat{T}_1 and \widehat{T}_2 is the sum of the squares of all these Frobenius norms between the remaining columns between \widetilde{T}_1 and \widetilde{T}_2 . In the example above, for $(1, 1, 0)^T$ of \widetilde{T}_1 , the closest column of \widetilde{T}_2 is $(1, 1, 1)^T$ and the difference is 1. For $(1, 1, 1)^T$ of \widetilde{T}_2 , the difference between $(1, 1, 0)^T$ is 1 and for $(0, 1, 1)^T$ of \widetilde{T}_2 , it is 2. The overall difference between \widehat{T}_1 and \widehat{T}_2 is then $1^2 + 1^2 + 2^2 = 6$. The measure of dissimilarity between two partially-joint structure matrix \widehat{T}_1 and \widehat{T}_2 is denoted $\text{diff}(\widehat{T}_1, \widehat{T}_2)$.

Finally, if the partially-joint structure $\widehat{\mathfrak{S}}_{0,1}$ (or $\widehat{\mathfrak{S}}_{0,2}$) has partially-joint structure matrices \widehat{T}_1 (or \widehat{T}_2), then the measure of dissimilarity between $\widehat{\mathfrak{S}}_{0,1}$ and $\widehat{\mathfrak{S}}_{0,2}$ is $\text{diff}(\widehat{\mathfrak{S}}_{0,1}, \widehat{\mathfrak{S}}_{0,2}) = \text{diff}(\widehat{T}_1, \widehat{T}_2)$.

B.2. Review on Methodology of Other Methods

We briefly review the methodology of AJIVE (Feng et al., 2018), SLIDE (Gaynanova and Li, 2019), COBS (Gao et al., 2021) and JIVE (Lock et al., 2013).

AJIVE In AJIVE, each signal matrix $Z_k \in \mathbb{R}^{p_k \times n}$ is regarded as a sum of joint structure J_k and individual structure I_k for $k = 1, \dots, K$. A joint structure J_k is viewed as the score subspace $[V_M] \in \mathbb{R}^n$ shared by all Z_i 's.

AJIVE extracts each estimated signal matrix \widehat{Z}_k from dataset X_k and \widehat{Z}_k is of initial rank estimate \widetilde{r}_k . The estimated shared joint component $[\widehat{V}_M]$ is obtained as a flag mean among score subspaces of \widehat{Z}_k 's, or $[\widehat{V}_1], \dots, [\widehat{V}_k]$, in a sense of the projection Frobenius norm distance as our method. The rank r_J

of $[\widehat{V}_M]$ (called the joint rank) is estimated using the simulated distribution of the largest singular value of the concatenated matrix of random directions and that of Wedin bounds:

- (1) If the largest squared singular value of the column concatenation matrix \widehat{V} of \widehat{V}_k 's is larger than the 5th percentile of the simulated distribution of the largest squared singular value of the concatenation matrix of random orthogonal matrices of the same size as \widehat{V}_k 's (or random direction bound), then $[\widehat{V}_M]$ is not generated by noise in 95 percent of probability.
- (2) If there are \widehat{r}_J squared singular values of \widehat{V} are larger than the 95th percentile of the simulated distribution of Wedin bounds, then the first \widehat{r}_J right singular vectors are used as the basis for the estimated joint score subspace $[\widehat{V}_M]$.

The estimated joint structure \widehat{J}_k is a projection of the dataset X_k onto the estimated joint score subspace $[\widehat{V}_M]$, that is, $\widehat{J}_k = X_k \widehat{V}_M \widehat{V}_M^T$. Each estimated individual structure \widehat{I}_k is obtained as $X_k \cdot (I - \widehat{V}_M \widehat{V}_M^T)$. The row spaces of each estimated individual structure \widehat{I}_k is orthogonal to $[\widehat{V}_M]$. There is no guarantee that individual structures are mutually orthogonal. The joint score matrix is just defined as \widehat{V}_M and the corresponding joint loading matrix for k th data source is a regression of \widehat{J}_k on \widehat{V}_M^T , computed as $\widehat{J}_k \cdot \widehat{V}_M$. The individual loading and score matrices are obtained from SVDs of \widehat{I}_k 's.

SLIDE SLIDE identifies the partially-joint structure with the penalized matrix factorization, that is,

$$(\widetilde{U}, \widetilde{V}) = \arg \min_{U, V} \sum_{k=1}^K \frac{1}{2} \|X_k - U_k V^T\|_F^2 + \lambda \sum_{j=1}^r \|U_{kj}\|_2 \quad \text{s.t. } V^T V = I,$$

where U_{kj} is the j th column of the loading matrix U_k of X_k and r is the number of all possible sparsity patterns. After computing \widetilde{U} and \widetilde{V} with an iterative algorithm, the corresponding structure matrix \widetilde{T} is obtained from the sparse structure of \widetilde{U} . Note that the concept of the structure matrix \widehat{T} here is identical to the partially-joint structure matrix of ours in Section B.1. Even though this optimization problem is nonconvex and there is no guarantee about convergence to the global optimum, authors reported that a local solution can be obtained heuristically by initializing V with the left singular matrix of concatenated X that works well in the simulation.

Then SLIDE estimate the loading and score matrices, \widehat{U} and \widehat{V} , for the structure \widehat{T} by solving the following optimization problem with an iterative algorithm,

$$(\widehat{U}, \widehat{V}) = \arg \min_{U, V} \|X - UV^T\|_F^2 \quad \text{s.t.} \quad V^T V = I,$$

with the constraint that the loading U has the same sparsity structure as \widehat{T} .

In model validation, SLIDE adapt the block cross validation (BCV) procedure to select the best structure $\widehat{T}_{\text{best}}$. BCV splits rows and columns of each dataset X_k into submatrices $X_k^{11}, X_k^{12}, \dots, X_k^{21}, \dots$. Then it holds out a set of submatrices $X^{ij} = [X_1^{ij}, X_2^{ij}, \dots, X_K^{ij}]$ of the same sub-block position in each dataset X_k and evaluate the prediction error on X^{ij} 's. Given a set of structure candidates $\widehat{T}_1, \widehat{T}_2, \dots$, we select one that minimizes the error across all folds.

JIVE Like in AJIVE, JIVE decompose each signal matrix X_i as a sum of joint structure J_i and individual structure I_i , for $i = 1, \dots, K$. After defining R to be a row concatenation of $R_i = X_i - J_i - I_i$, JIVE estimate both joint and individual structures by minimizing $\|R\|_F^2$ under the given ranks. An alternating iterative algorithm is implemented for the estimation finding individual component with given joint component at one step and vice versa at another step. The estimated joint structure is identical to the first r_J terms in the SVD of X with individual components removed and the estimated individual structures to the first r_i terms in the SVD of X_i with the joint component removed. The selection of r_J and r_i 's are validated using the permutation test.

COBS COBS iteratively estimates a sequence of loading vectors, u_i for $i = 1, \dots, r$ for given r , while updating the data matrix $X = [X_1, \dots, X_k] \in \mathbb{R}^{n \times \sum p_k}$. The algorithm starts with $X^{[0]} = X$. At the i th step, with the current data matrix $X^{[i-1]}$, the i th loading vector u_i is estimated solving the following maximization problem, that is,

$$\tilde{u}_i = \max_u \|(X^{[i-1]})^T u\|_2^2 \quad \text{s.t.} \quad u^T u = 1.$$

As each u_i is equipped with block structure $u_i = \left(u_{(1)}^T \dots u_{(K)}^T \right)^T$, we can give sparsity at two levels of thresholding, one for block-wise sparsity and the other for overall sparsity in estimating \tilde{u}_i . The tuning parameters $\alpha_v \in [0, 1]$ and $\lambda_v \geq 0$ control the two levels of sparsity respectively, and \widehat{u} is thresholded

as a normalized solution of

$$\min_x \frac{1}{2} \|x - \tilde{u}_i\|^2 + \gamma_1 \|x\|_1 + \gamma_2 \|x\|_{2,1},$$

where $\gamma_1 = \alpha_v \lambda_v$ and $\gamma_2 = (1 - \alpha_v) \lambda_v$. Then the score vector v_i is estimated as the empirical BLUP and dataset $X^{[i-1]}$ is updated as $X^{[i]} = X^{[i-1]} - \hat{u}_i \hat{v}^T$.

B.3. Computation time comparison

Table B.5: Time comparison among our method and other four method(SLIDE, COBS, AJIVE and JIVE). The computation time reported. The unit is second(s). Averages and standard deviations are over 10 replications

Model	SNR	PSI-MDI	SLIDE bcr	COBS	AJIVE	JIVE
1	10	0.88 (0.13)	2.66 (0.1)	10.05 (0.05)	11.43 (0.02)	5.71 (0.05)
	5	0.79 (0.00)	3.41 (0.14)	10.97 (0.06)	11.44 (0.02)	5.72 (0.04)
2	10	1.01 (0.21)	1.05 (0.03)	4.39 (0.05)	11.44 (0.02)	21.82 (6.68)
	5	0.93 (0.01)	0.87 (0.03)	3.85 (0.04)	11.45 (0.01)	20.52 (4.74)
3	10	1.72 (0.15)	3.58 (0.08)	10.6 (0.05)	11.23 (0.02)	58.33 (19.05)
	5	1.5 (0.01)	4.87 (0.16)	10.45 (0.06)	11.23 (0.04)	34.83 (0.02)
4	10	1.5 (0.14)	4.36 (0.16)	14.47 (0.04)	11.28 (0.06)	26.28 (13.47)
	5	1.23 (0.07)	5.91 (0.24)	14.1 (0.05)	11.26 (0.02)	33.27 (22.91)
5	10	2.48 (0.13)	5.73 (0.19)	13.45 (0.06)	11.1 (0.04)	61.81 (30.06)
	5	1.91 (0.06)	8.87 (0.23)	13.15 (0.05)	11.31 (0.42)	36.43 (6.58)
6	10	2.88 (0.13)	10.75 (0.31)	24.14 (0.07)	11.08 (0.21)	22.58 (0.04)
	5	2.01 (0.07)	22.82 (0.72)	27.61 (0.05)	10.99 (0.02)	43.93 (8.81)

B.4. Results on Tuning Parameter Selection

We report the performances of our tuning parameter selection procedure of Section 3.3 using the six models given in Section 5. Since the tuning parameter λ represents a threshold for principal angles, the candidates for λ are given by $\lambda = 0^\circ, 1^\circ, \dots, 90^\circ$. For each value of λ , we evaluated the empirical risk. As discussed in Section 3.3, we take the parameter $\tilde{\lambda}$ that gives the smallest empirical risk and also compare $\text{diff}(\widehat{\mathfrak{S}}_0(\tilde{\lambda}_0; \widehat{Z}_{tr}), \widehat{\mathfrak{S}}_0(\lambda; \widehat{Z}))$ as a function of λ . We also present $\text{diff}(\widehat{\mathfrak{S}}_0(\lambda, \widehat{Z}), \mathfrak{S}_0)$, which reflects how much the estimated structure differs from the true structure on each value of angle threshold, under the situation where the true structure (‘oracle’) is known.

When SNR = 10, `getnfrac` function estimated true signal ranks correctly for models 1 to 5. The empirical risk is minimized at an interval of λ 's, and for any λ in the interval, the corresponding structure $\widehat{\mathfrak{S}}_0$ matches the true \mathfrak{S}_0 ; the valley bottoms of empirical risk (solid line) are posited inside those of the measure of dissimilarity (dashed line) with value zero, as seen in Fig. B.6. For each model in the figure, solid line (empirical risk) shows a similar shape as dashed line (the measure of dissimilarity), which implies that empirical risk well reflects the difference between the estimated structure and the true

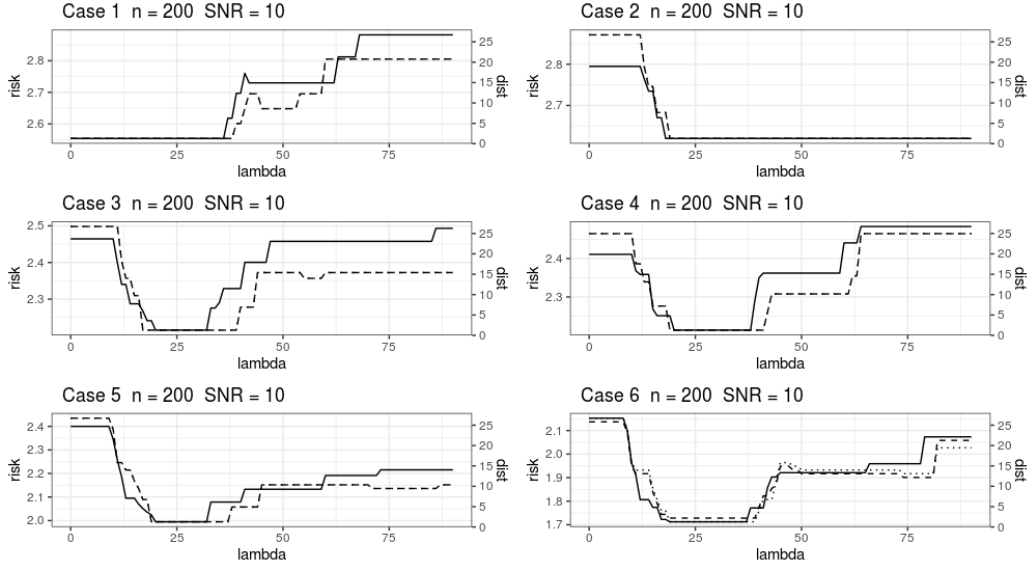


Figure B.6: The values of empirical risk (solid) and $\text{diff}(\widehat{\mathfrak{S}}_0(\tilde{\lambda}_0; \widehat{Z}_{tr}), \widehat{\mathfrak{S}}_0(\lambda; \widehat{Z}))$ (dotted), $\text{diff}(\widehat{\mathfrak{S}}_0(\lambda, \widehat{Z}), \mathfrak{S}_0)$, (dashed).

structure. In Model 6, the true signal rank is 8 for each dataset, for instance, from $\{(\{1, 2, 3\}, 2), (\{1, 2\}, 2), (\{1, 3\}, 2), (\{1\}, 2)\}$ in the case X_1 . However, `getnfrac` function only estimated $r_1 = 8$, $r_2 = 8$ and $r_3 = 7$. The estimated partially-joint structure lacks $(\{3\}, 1)$ from the true structure.

When the signal-to-noise ratio is small, $\text{SNR} = 2$, `getnfrac` function estimated signal ranks as zero for all six cases, so we give the true inherent signal ranks instead. Unfortunately, the empirical risk is minimized at smaller values of λ than desired; see Fig. B.7. Unlike Fig. B.6, solid line (empirical risk) shows a far different shape than dashed line (the measure of dissimilarity), except for Model 1, which implies that empirical risks fail to detect the true structure. This is due to the lower value of SNR, with which the magnitude of noise overwhelms that of signal. As the score vectors of each dataset have almost random directions in low SNRs, there is a tendency that signals from a partially-joint (and fully-joint) scores are counted separately as if they belong to individual data blocks.

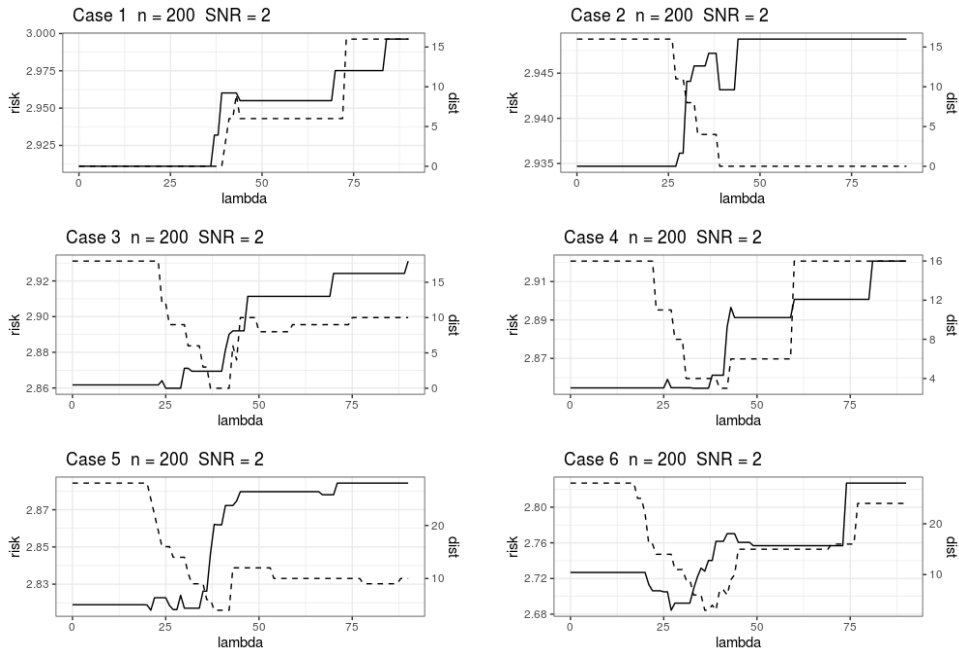


Figure B.7: The values of penalized empirical risk for λ when $n = 200$ and $\text{SNR} = 2$. The values of empirical risk (solid line) and the measure of dissimilarity, $\text{diff}(\hat{\mathfrak{G}}_0(\lambda, \hat{Z}), \mathfrak{G}_0)$, (dashed line) over varying λ are shown.

B.5. Simulation Settings for Section 5.4

In the unbalance of signal strength between joint and individual component settings, we set $n = 200$ and $K = 3$.

In the first case, we set the elements of σ_M^2 as

- (1) Joint (S_1) : (15, 14.5, \dots , 5.5),
- (2) Individual 1 (S_2) : (0.150, 0.141, 0.132, \dots , 0.069),
- (3) Individual 2 (S_3) : (0.147, 0.138, 0.129, \dots , 0.066),
- (4) Individual 3 (S_4) : (0.144, 0.135, 0.126, \dots , 0.063),

so the strength of joint signals are about 100 times stronger than those of individual signals.

In the second case case, we set the elements of σ_M^2 as

- (1) Joint (S_1) : (0.15, 0.145, \dots , 0.055),
- (2) Individual 1 (S_2) : (15, 14.1, 13.2, \dots , 6.9),
- (3) Individual 2 (S_3) : (14.7, 13.8, 12.9, \dots , 6.6),
- (4) Individual 3 (S_4) : (14.4, 13.5, 12.6, \dots , 6.3),

so the strength of individual signals are about 100 times stronger that those of joint signals.

C. Additional Information on Real Data Analysis

Table C.1: Fisher’s exact tests between gene mutations/chromosome defects and the CLL subgroups, α and β were conducted simultaneously. The p-values were adjusted with the FDR (Benjamini-Hochberg method) and the top 5 lowest FDR (BH method) adjusted p-values were listed.

Gene mutation/Chromosome defect	adjusted p-value
IGHV	1.036×10^{-13}
MED12	0.173
del17p13	0.174
del13q14	0.178
TP53	0.184

Table C.2: The association between IGHV mutation status and the CLL subgroups with an FDR (BH method) adjusted p-value 1.036×10^{-13} from the Fisher’s exact test. Nine missing data for IGHV mutation status were excluded.

Mutation \ Subgroup	α	β
IGHV Wild type	49	8
IGHV Mutated	7	48

Table C.3: The most appeared drugs in the subgroups [a] and [b] with appearances at least four times out of 5 concentrations.

The most appeared drugs in subgroup [a]		
Drug name	Target pathway	Appearances
spebrutinib	BTK	5
idelalisib	PI3K delta	5
duvelisib	PI3K gamma, PI3K delta	5
tamatinib	SYK	5
dasatinib	ABL1, KIT, LYN, PDGFRA, PDGFRB, SRC	5
PF 477736	CHK1, CHK2	5
MK-2206	AKT1/2 (PKB)	5
ibrutinib	BTK	4
selumetinib	MEK1/2	4
PRT062607 HCL	SYK	4
AZD7762	CHK1/2	4
CCT241533	CHK2	4
TAE684	ALK	4
MK-1775	WEE1	4
AT13387	HSP90	4

The most appeared drugs in the subgroup [b]		
Drug name	Target pathway	Appearances
everolimus	mTOR	5
thapsigargin	SERCA	5
orlistat	LPL	5
rotenone	Electron transport chain in mitochondria	5
afatinib	EGFR, ERBB2	4
fludarabine	Purine analogue	4
navitoclax	BCL2, BCL-XL, BCL-W	4

References for Supplementary Materials

- Feng, Q., Jiang, M., Hannig, J., Marron, J., 2018. Angle-based joint and individual variation explained. *Journal of Multivariate Analysis* , 241–265.
- Gao, X., Lee, S., Jung, S., 2021. Covariate-driven factorization by thresholding for multi-block data. *Biometrics* 77(3), 1011–1023.
- Gaynanova, I., Li, G., 2019. Structural learning and integrative decomposition of multi-view data. *Biometrics* 75, 1121–1132.
- Lock, E., Hoadley, K., Marron, J., Nobel, A., 2013. Joint and individual variation explained (jive) for integrated analysis of multiple data types. *Annals of Application Statistics* 7(1), 523–542.